Science and Technology of Advanced Materials

ISSN: 1468-6996 (Print) 1878-5514 (Online) Journal homepage: www.tandfonline.com/journals/tsta20

Reproducible chiroptical activity from aggregated chiral thienopyrroledione–fluorene π-conjugated polymers

Nao Suzuki, Ziwei Hu, Sota Nakayama, Soh Kushida, Yohei Yamamoto, Wijak Yospanya, Reiko Oda, Takaki Kanbara & Junpei Kuwabara

To cite this article: Nao Suzuki, Ziwei Hu, Sota Nakayama, Soh Kushida, Yohei Yamamoto, Wijak Yospanya, Reiko Oda, Takaki Kanbara & Junpei Kuwabara (02 Jun 2026): Reproducible chiroptical activity from aggregated chiral thienopyrroledione–fluorene π-conjugated polymers, Science and Technology of Advanced Materials, DOI: 10.1080/14686996.2026.2680968

To link to this article: https://doi.org/10.1080/14686996.2026.2680968

Publisher: Taylor & Francis & The Author(s). Published by National Institute for Materials Science in partnership with Taylor & Francis Group.

Journal: *Science and Technology of Advanced Materials*

DOI: 10.1080/14686996.2026.2680968

Reproducible chiroptical activity from aggregated chiral thienopyrroledione–fluorene π-conjugated polymers.

Nao Suzuki,[a] Ziwei Hu,[a] Sota Nakayama,[a] Soh Kushida,[a] Yohei Yamamoto,[a,b] Wijak Yospanya,[c] Reiko Oda,[d,c] Takaki Kanbara,[a] Junpei Kuwabara[a,b] *

[a] *Institute of Pure and Applied Sciences, University of Tsukuba 1-1-1 Tennodai, Tsukuba, Ibaraki 305-8573, Japan.*

[b] *Tsukuba Research Center for Energy Materials Science (TREMS), Institute of Pure and Applied Sciences, University of Tsukuba, 1-1-1 Tennodai, Tsukuba, Ibaraki 305-8573, Japan.*

[c] *Advanced Institute for Materials Research (AIMR), Tohoku University, 2-1-1 Katahira, Aoba, Sendai, Miyagi, Japan*

[d] *University of Bordeaux, CNRS, Bordeaux INP, CBMN, UMR 5248, F-33600 Pessac, France*

E-mail: kuwabara@ims.tsukuba.ac.jp

Abstract

Chiral π-conjugated polymers have attracted considerable interest because their chiral aggregated structures can generate pronounced chiroptical responses. Here, we report the design, synthesis, and chiroptical characterization of fluorene–thienopyrroledione polymers bearing a single chiral center in each repeating unit, **(*R*)-** and **(*S*)-PFTPD**, prepared *via* direct arylation polycondensation to minimize structural defects. Although only weak chiroptical activity was observed in a solution, addition of 1-butanol to $CHCl_3$ solutions of the polymers induced the formation of stable aggregates that exhibited strong circular dichroism (CD) and circularly polarized luminescence (CPL). Systematic examination of the sample preparation parameters revealed that the mixing process critically influences the chiroptical properties. Dropwise addition of 1-butanol under controlled stirring provided the most reliable results, yielding highly reproducible CD spectra. Under these optimized conditions, the aggregates exhibited an average dissymmetry factor ($|g_{abs}|$) of 1.5×10^{-2} and a CPL dissymmetry factor ($|g_{lum}|$) of 1.9×10^{-2}. These values rank among the highest reported for π-conjugated polymer aggregates

bearing only a single chiral source per repeat unit. This study demonstrates that precise control over the solvent-mixing process is essential for the reproducible emergence of chiroptical properties and highlights the chiral TPD unit as a promising platform for chiroptical polymer materials.

Keywords: chiral π-conjugated polymer, thienopyrroledione, circular dichroism, circularly polarized luminescence

Impact Statement: This study demonstrates highly reproducible, strong CD and CPL from chiral π-conjugated polymers, enabled by a robust and standardized aggregate-formation protocol.

Introduction

Chirality is a fundamental structural motif that manifests across multiple length scales from molecular to supramolecular and even macroscopic dimensions, and plays a key role in determining the properties of functional organic materials. In π-conjugated systems, the combination of extended electronic delocalization and chiral organization offers unique opportunities for controlling light–matter interactions, enabling phenomena such as circular dichroism (CD) and circularly polarized luminescence (CPL) [1,2]. The chiroptical

properties of π-conjugated materials are governed not only by their intrinsic molecular asymmetry but also, and often predominantly, by their supramolecular organization in thin films or aggregated states [3–5]. Chiral side-chain–functionalized π-conjugated polymers such as poly(*p*-phenylene)s [6–8], poly(*p*-phenylene-vinylene)s [9], and polythiophenes [10, 11] have long been studied for their chiroptical properties. In particular, π-conjugated polymers containing fluorene units exhibit distinctive optical activity arising from their unique aggregation behavior and liquid-crystalline ordering [12–19]. The fluorene unit's rigid backbone and strong propensity for self-organization, combined with precise control over intermolecular packing through 9,9-disubstitution (Figure 1a), underlie these distinctive chiroptical properties. Introduction of chiral side chains onto fluorene units has been recognized as a key strategy for generating pronounced CD and CPL responses [17]. Nevertheless, the reliance on conventional chiral building blocks limits the accessible structural diversity. In contrast, the thienopyrroledione (TPD) unit offers a highly versatile platform for molecular design (Figure 1b) [20]. Because its substituent can be directly derived from primary amines, a wide variety of readily available chiral amines can be seamlessly incorporated as chiral side chains. This straightforward and modular approach greatly expands the accessible library of chiral monomers, enabling systematic tuning of molecular asymmetry and facilitating the creation of structurally diverse chiral conjugated

polymers. Moreover, TPD is a strong electron-accepting unit known to impart high chemical stability, distinctive aggregation behavior, and suitability for use in organic semiconducting polymers [20, 21]. For an accurate understanding of the intrinsic chiroptical properties of chiral polymers, it is also crucial to prepare polymers with minimal structural defects along the main chain. We have previously demonstrated that π-conjugated polymers containing TPD can be synthesized *via* direct C–H arylation polycondensation [22–25], enabling precise control over backbone structure and chain ends [26, 27]. When properly optimized, this method affords defect-free polymers more efficiently than conventional cross-coupling polymerizations and is therefore highly suitable for fundamental studies on chiral conjugated systems. In this work, we designed and synthesized chiral TPD monomers derived from chiral amines and prepared copolymers with achiral dioctyl-substituted fluorene units *via* direct arylation polycondensation. By systematically investigating their CD and CPL responses, we aimed to elucidate the role of the chiral TPD unit in governing the chiroptical properties of the resulting polymers. During this investigation, we encountered significant issues in the reproducibility of the chiroptical responses. To overcome this issue, we established an experimental protocol that enables highly reproducible observation of CD and CPL responses from the polymers. Notably, this protocol directly addresses a critical challenge

common to aggregated and solid-state chiral π-conjugated systems, namely the poor reproducibility of chiroptical responses arising from subtle differences in sample preparation and processing conditions [3, 9, 28–30]. Despite containing only a single chiral source within each repeating unit, the polymers exhibited CPL dissymmetry factors on the order of 10^{-2} in the aggregated state. These values are an order of magnitude larger than those typically reported for polymer aggregates dispersed in solution ($\sim 10^{-3}$). These findings demonstrate that the chiral TPD unit is highly effective in inducing supramolecular chirality and provides a new molecular-design principle for chiral π-conjugated polymers.

<Figure 1.>

Results and discussion

Synthesis and characterization of polymers.

In this study, (*R*)-1-cyclohexylethylamine was selected from among readily accessible chiral amines. This choice was motivated by the fact that the chiral center is positioned directly adjacent to the nitrogen atom, allowing it to be placed in close proximity to the

polymer backbone when incorporated into the TPD unit. Such proximity is expected to enable the TPD side chain to more effectively influence the chiral organization of the polymer through intermolecular π–π stacking upon aggregation. In addition, the cyclohexyl group ensures sufficient solubility of the polymer. The TPD bearing the (*R*)-1-cyclohexylethyl side chain, **(*R*)-TPD**, was synthesized following the synthetic procedure reported for the corresponding achiral side-chain derivative (Scheme 1a) [31]. After converting 3,4-thiophenedicarboxylic acid to the corresponding anhydride, the intermediate was reacted with (*R*)-1-cyclohexylethylamine without isolation, followed by dehydration to afford the desired product in an overall yield of 69%. The obtained compound was characterized by ^{1}H and ^{13}C NMR spectroscopy, mass spectrometry, and elemental analysis. Using ^{1}H-^{1}H COSY NMR in combination with a DFT-calculated chemical-shift prediction, all signals observed in the ^{1}H NMR spectrum were fully assigned (Figure S1-S3). The three-dimensional structure was ultimately elucidated by single-crystal X-ray diffraction analysis (Figure 2). Two crystallographically non-equivalent molecules were present in the unit cell, and one of the cyclohexyl groups exhibited disorder. Figure 2 shows the structure without the disordered component. Both the cyclohexyl and methyl groups adopt orientations above and below the TPD plane, respectively, presumably to minimize steric repulsion.

<Scheme 1.>

<Figure 2.>

When the direct arylation polycondensation between **(*R*)-TPD** and 9,9-dioctyldibromofluorene was conducted under the optimized conditions (Scheme 1b) [27], **(*R*)-PFTPD** was obtained in 94% yield with an M_n of 45,000 (Table 1). The structure of the obtained polymer was confirmed by ^{1}H NMR spectroscopy and matrix-assisted laser desorption/ionization time-of-flight mass spectrometry (MALDI-TOF MS) (Figures S4 and S5). The MALDI-TOF-MS spectrum of **(*R*)-PFTPD** indicates the absence of structural defects such as homocoupling, and shows that most chain termini are capped with the TPD unit. The presence of the TPD terminal group is also confirmed by the ^{1}H NMR spectrum (Figure S4).

<Table 1.>

The enantiomeric **(*S*)-TPD** and **(*S*)-PFTPD** were synthesized in the same manner. The obtained monomers and polymers exhibited nearly identical NMR and MALDI-TOF MS spectra (Figure S6-S8). In addition, **(*R*)-PFTPD** and **(*S*)-PFTPD** exhibit comparable molecular weights (Table 1). These results allow direct comparison of their chiral properties without contributions from differences in structural defects or molecular weights. The polymer was confirmed to be amorphous, as evidenced by the absence of distinct diffraction peaks in the X-ray diffraction (XRD) pattern and the lack of any crystallization- or melting-related thermal transitions in the differential scanning calorimetry (DSC) thermograms (Figures S9 and S10).

Photophysical properties in solution and film states

To investigate the fundamental physical properties of the polymers, absorption and photoluminescence spectra were measured in both solution and thin-film states (Figure S11). In solution, the polymer showed a maximum absorption at 463 nm and an emission maximum at 487 nm (Table 1). Time-dependent density functional theory (TD-DFT) calculations indicate that the longest-wavelength absorption band originates from a π–π transition along the polymer backbone (Figure S12). The absorption and emission spectra of the spin-coated thin films were slightly red-shifted (λ_{abs} = 465 nm, λ_{em} = 495 nm)

relative to those observed in solution, suggesting that solid-state packing causes only slight modifications to the electronic states (Figure S11b).

Chiroptical properties and reproducibility

The chiroptical properties were evaluated using circular dichroism (CD) spectroscopy. In $CHCl_3$ solution, only a very weak CD signal was observed at a repeating-unit concentration of 3.0×10^{-5} M for **(*R*)-PFTPD**, consistent with the similarly weak CD activity observed for the corresponding chiral monomer, **(*R*)-TPD** (Figure S13). These results indicate that the individual chiral centers do not generate sufficient coupling between electric and magnetic transition dipole moments to produce strong CD signals in the solution state, as commonly observed for other conjugated polymers [3,6,8,9]. To promote aggregation, 1-butanol was introduced as a poor solvent. The resulting aggregates remained stably dispersed for more than 48 hours (Figure S14). When various solvent ratios were examined, a strong CD signal was observed at a $CHCl_3$/1-butanol volume ratio of 40:60. Notably, examination of the reproducibility revealed that the CD intensities varied by more than an order of magnitude depending on the sample preparation conditions (Table S1). Such variations in CD and CPL intensities arising from differences in preparation methods or processing procedures have also been reported previously [9].

These observations underscore the importance of reproducibility in the chiroptical properties of the aggregates and motivated us to identify the key factors required to obtain consistent and reliable results. When 1-butanol was slowly added to the polymer solution in $CHCl_3$, thereby allowing the two solvents to diffuse gradually, the resulting sample exhibited small $|g_{abs}|$ values (average: 1.4×10^{-3}, Table 2, Condition 1). One-shot addition of 1-butanol to the polymer solution, followed by manual shaking to promote mixing of the two solvents, resulted in a high $|g_{abs}|$ value of 7.0×10^{-3}; nevertheless, the reproducibility was low, as indicated by a large standard deviation (± 0.0054) (Condition 2). When 1-butanol was added dropwise to the polymer solution in $CHCl_3$ under stirring, even higher $|g_{abs}|$ values 1.5×10^{-2} were obtained; however, the reproducibility remained unsatisfactory (Condition 3). By standardizing the stirring speed of the polymer solution (450 rpm), highly reproducible $|g_{abs}|$ values with small standard deviation (± 0.0028) were obtained (Condition 4). Although both Conditions 3 and 4 employed dropwise addition under stirring, controlling the stirring speed proved essential for ensuring rapid and reproducible mixing, which substantially improved the reproducibility of the $|g_{abs}|$ values. Collectively, these results demonstrate that the manner in which the polymer solution in $CHCl_3$ is mixed with the poor solvent 1-butanol plays a crucial role in determining the chiroptical properties of the aggregates. In particular, controlled stirring during solvent mixing

(Condition 4) enables highly reproducible aggregate formation and was therefore adopted for subsequent measurements (Figure 3).

<Table 2.>

<Figure 3.>

The pronounced dependence of the chiroptical properties on the sample preparation process suggests that the aggregation pathway plays a decisive role in defining the structure of the aggregates. In film or aggregated states, chromophores are brought into close spatial proximity, enabling intermolecular exciton coupling that strongly enhances CD responses, as widely observed for chiral π-conjugated systems [3, 28]. The magnitude and shape of these exciton-coupled CD signals are therefore highly sensitive to the molecular arrangement established during aggregation [29]. In this context, Koeckelberghs and co-workers demonstrated that conjugated polymers bearing chiral side chains can follow distinct aggregation pathways depending on the rate of poor solvent addition, yielding kinetically trapped or thermodynamically stabilized structures with markedly different chiroptical properties [30]. Notably, their study showed that rapid aggregation favors a kinetically controlled, π–π-stacking-dominated structure that produces stronger

CD signals, whereas slower aggregation allows relaxation into thermodynamically preferred assemblies exhibiting lower CD intensity. The behavior observed in the present **PFTPD** system is consistent with these trends. When 1-butanol was introduced under controlled stirring to ensure rapid and homogeneous mixing, the polymers formed kinetically favored aggregates exhibiting the largest CD amplitudes (Condition 4). In contrast, slow diffusion-controlled aggregation resulted in significantly weaker CD responses (Condition 1), suggesting that the aggregates formed under such conditions adopt less cooperative chiral arrangements. The sensitivity of the CD intensity to the specific mixing protocol therefore supports the view that the strongest chiroptical responses arise from kinetically trapped aggregates, whose local packing geometry maximizes exciton coupling among **PFTPD** chromophores. Different aggregation pathways can, in principle, lead to distinct CD patterns; however, the CD spectra obtained under different mixing conditions (Conditions 1 and 4) exhibited similar spectral shapes, with variations observed only in their intensities (Figure S15). This indicates that the characteristic CD pattern originates from kinetically formed aggregates, whereas the thermodynamically favored aggregates are largely CD-inactive. Under slow aggregation conditions (Condition 1), the reduced CD intensity is therefore attributed to an increased fraction of CD-inactive aggregates. Collectively, these results reaffirm that the aggregation

pathway strongly influences the chiroptical properties. Moreover, strict control over the preparation conditions is indispensable for achieving reproducible chiroptical responses. Our findings particularly underline the necessity of precisely controlling and explicitly reporting solvent addition and mixing protocols to enable reliable comparison of chiroptical data across studies.

Effects of solvent ratio on chiroptical properties

CD spectra of **(*R*)-PFTPD** and **(*S*)-PFTPD** were measured in solvent mixtures with varying $CHCl_3$/1-butanol ratios using samples prepared by an optimized solvent mixing protocol (Condition 4) to ensure reproducibility. When the volume fraction of 1-butanol was below 50%, the CD intensity remained low. Figure 4 shows the UV–Vis absorption and CD spectra obtained when the volume fraction of $CHCl_3$ relative to 1-butanol was decreased from 50:50 to 30:70. It should be noted that no precipitation was observed at any of these solvent ratios (Figure S14). At the volume ratio of $CHCl_3$ to 1-butanol of 50:50, the absorption spectrum is similar to that in pure $CHCl_3$, and the CD signal intensity is still low (Figure 4). These observations indicate that most of the polymer remains soluble at this solvent ratio. Upon changing the solvent ratio to 40:60, the intensity of the absorption band around 450 nm decreased, and the overall spectrum became

broadened, indicating polymer aggregation. At this ratio, the aggregates exhibit a bisignate CD signal in the absorption region, accompanied by a pronounced increase in CD intensity (Figure 4b). As the CD intensity decreases at the 30:70 ratio, the 40:60 mixture represents the solvent ratio with the highest chiroptical response. In terms of g_{abs}, the sample in the 40:60 mixture showed the highest value, with a g_{abs} of -1.6×10^{-2} at 491 nm (Figure S16, Table S2). For all three solvent ratios examined, the CD spectra of **(*R*)-PFTPD** and **(*S*)-PFTPD** were approximately mirror images of each other (Figure S17). The observed deviation from an ideal mirror-image relationship is attributed to unavoidable technical variations in the sample preparation process.

<Figure 4.>

Characterization of Aggregates

As the chiroptical properties vary depending on the solvent ratio, the corresponding aggregates were examined by optical microscopy and scanning electron microscopy (SEM) (Figure 5). When the aggregates dispersed in each solvent were observed under an optical microscope under blue–violet light irradiation, numerous fine particles exhibiting yellow-green emission were detected in a 50:50 solvent mixture (Figure 5a). In contrast,

relatively large aggregates were observed in the 40:60 and 30:70 mixtures (Figure 5b and 5c). To examine the morphological differences in detail, SEM observations were performed. In the sample prepared from the 50:50 solvent mixture, film-like deposits were observed on the substrate (Figure 5d). Given that most polymers are dissolved in a 50% $CHCl_3$ mixture solvent, it is expected these dissolved polymers precipitate to form a thin film on the substrate in a drying process. The SEM image of the sample prepared in the 40:60 mixed solvent reveals that the aggregates consist of very small, interconnected particles (Figure 5e). In contrast, the sample prepared in the 30:70 mixed solvent shows aggregates with a smooth surface morphology (Figure 5f). Because SEM measurements were carried out after solvent evaporation, the observed morphologies do not necessarily represent the aggregate structures present in dispersion. Nevertheless, qualitative differences in surface morphology were observed among samples prepared at different solvent ratios. Notably, aggregates formed at the 40:60 $CHCl_3$/1-butanol ratio showed a distinct fine particulate morphology, which was not clearly observed under the other conditions.

<Figure 5.>

CPL properties.

In a 40:60 mixed solvent of $CHCl_3$ and 1-butanol, **(*R*)-** and **(*S*)-PFTPD** exhibit emission spectra with maxima at 500 nm (Figure 6). The photoluminescence quantum yield was determined to be 33%, which is relatively high for aggregates of conjugated polymers. Aggregates of **(*R*)-PFTPD**s in the mixed solvents exhibited a CPL signal with a g_{lum} of -1.7×10^{-2} at 500 nm, while **(*S*)-PFTPD** gave a mirror-image CPL signal of opposite sign. For this solvent ratio, measurements were performed on six independently prepared samples, yielding an average $|g_{lum}|$ value of 1.9×10^{-2} with a standard deviation of 4.9×10^{-3}, demonstrating good reproducibility (Table S3). In general, conjugated polymers bearing chiral side chains typically exhibit g_{lum} values on the order of 10^{-3} in solution and for aggregated samples in poor solvents [32–40]. In this context, the g_{lum} values on the order of 10^{-2} observed in the present system are notable for solution-based polymer aggregates prepared without long-range structural ordering. Previous studies have demonstrated that exceptionally large g_{lum} values approaching 10^{-1} can be realized in highly ordered interchain helically π-stacked polymer assemblies, achieved by combining cationic polymers with suitably designed anionic π-conjugated molecules to precisely control π–π interactions.[7] By contrast, the present system relies on a minimal molecular design, yet still affords g_{lum} values on the order of 10^{-2}, underscoring the effectiveness of

the chiral TPD unit in promoting supramolecular chirality upon aggregation.

<Figure 6.>

Conclusion

In conclusion, we have shown that the thienopyrroledione (TPD) unit bearing a chiral side chain functions as an effective chiral building block for π-conjugated polymers, enabling pronounced chiroptical activity upon aggregation. Direct arylation polycondensation afforded structurally well-defined fluorene–TPD polymers with a single chiral center per repeat unit, allowing their intrinsic properties to be assessed without interference from structural defects. Although CD activity in solution was weak, mixing $CHCl_3$ solutions with 1-butanol produced stable aggregates displaying strong CD and CPL responses. Systematic evaluation of the preparation conditions revealed that the solvent mixing protocol plays a decisive role in both the emergence and reproducibility of chiroptical activity. The addition of the poor solvent under controlled stirring produced the most consistent aggregates, yielding reproducible $|g_{abs}|$ and $|g_{lum}|$ values of 1.5×10^{-2} and 1.9×10^{-2}, respectively—remarkably high considering that each repeat unit contains only a single chiral center. Such preparation conditions should be precisely controlled and

explicitly reported in studies of self-assembled chiroptical systems. Furthermore, the strong dependence of the CD intensity on the mixing method is consistent with a pathway in which kinetically trapped aggregates maximize exciton-coupled chiroptical enhancement among PFTPD chromophores. This study demonstrates that the chiral TPD unit inherently possesses a high potential for inducing strong chiroptical responses, which can be fully realized through precise control of the aggregation process.

Experimental

^{1}H and $^{13}C\{^{1}H\}$ NMR spectra were recorded using Bruker AVANCE-400 NMR spectrometer and AVANCE-600 NMR spectrometer. Tetramethylsilane was used as an internal standard (0 ppm) for ^{1}H and $^{13}C\{^{1}H\}$ NMR spectra. Elemental analyses were carried out using an elementar UNICUBE. Intensity data for crystal structure determination were collected on a Rigaku XtaLAB Synergy-R with Cu Kα radiation. The crystal used for analysis was prepared from a concentrated hexane solution of **(*R*)-TPD**. The crystal was mounted using MicroMounts (MiTeGen). Crystallographic data for **(*R*)-TPD** have been deposited with the Cambridge Crystallographic Data Centre as supplementary publication CCDC 2533781. UV-Vis absorption spectra were recorded on a Hitachi U-3900H with a

scan speed of 300 nm min^{-1} and a slit width of 2 nm or JASCO V630 spectrophotometer with a scan speed of 400 nm min^{-1} and a slit width of 1.5 nm. Photoluminescence spectra were recorded on a Hitachi F-2700 fluorescence spectrophotometer with an excitation slit width of 10.0 nm, an emission slit width of 10.0 nm, a photomultiplier tube voltage of 400 V, a response time of 0.08 s, and a scan speed of 1500 nm min^{-1}. The PL quantum yields (PLQY) were measured using a Hamamatsu Photonics C9920-02 absolute PL quantum yield spectrometer. CD measurements were carried out by JASCO J820 with the sensitivity set to low, a scan speed of 50 nm min^{-1}, a response time of 1 s, and a bandwidth of 1 nm. Measurements were performed in continuous scanning mode at 25 °C with stirring. CPL measurements were carried out by JASCO CPL-300 with an excitation wavelength of 400 nm, an excitation bandwidth of 10.0 nm, and an emission bandwidth of 16.0 nm. Measurements were performed in continuous scanning mode at a scan speed of 100 nm min^{-1}, with a photomultiplier tube voltage of 700 V, at 25 °C under stirring at 600 rpm, with five accumulations. The CD and CPL properties of the polymers were evaluated in solution at a repeating-unit concentration of 3.0×10^{-5} M. An X-ray diffraction pattern was recorded at 298 K on a Rigaku model MultiFlex X-ray diffractometer with a CuKα radiation source. The thermal properties were measured on an EXSTAR7000 DSC instrument. MALDI-TOF-MS spectra were recorded on a Shimadzu AXIMA-CFR Plus.

Fluorescence microscopy observations were carried out using an Olympus model BX53 upright microscope. Scanning electron microscopy (SEM) was performed on a Hitachi Model S-3700N SEM operating at 15 kV. Dry solvents were purchased from Kanto Chemical. $Pd(OAc)_2$ (Kojima Chemicals Co., Ltd.) was used as a catalyst. The other reagents were purchased from Tokyo Chemical Industry Co., Ltd. (TCI), Sigma-Aldrich and FUJIFILM Wako Pure Chemical Corporation. DFT calculations were performed at the B3LYP/6-31G(d) level using Gaussian 16 package.

Synthesis

Synthesis of (*R*)-5-(1-cyclohexylethyl)-4*H*-thieno[3,4-*c*]pyrrole-4,6(5*H*)-dione, (**(*R*)-TPD**).

A 25 mL Schlenk tube charged with a magnetic stir bar was loaded with 3,4-thiophenedicarboxylic acid (172.2 mg, 1.0 mmol) and acetic anhydride (3.23 mL), and the mixture was refluxed at 140 °C for 6 h. After cooling to room temperature, the reaction mixture was dried under vacuum. toluene (3.23 mL) and (*R*)-1-cyclohexylethylamine (219 μL, 1.5 mmol) were added, and the mixture was refluxed at 120 °C for 24 h under a nitrogen atmosphere. After cooling to room temperature, the mixture was dried under vacuum. Thionyl chloride (1.1 mL) was then added, and the mixture was refluxed at 72 °C

for 3 h under a nitrogen atmosphere. After cooling to room temperature, the reaction mixture was dried under vacuum. The resulting solid in the Schlenk tube was extracted with *n*-hexane, washed three times with distilled water and once with saturated brine. The organic layer was dried over Na_2SO_4 and concentrated under reduced pressure. The crude product was purified by silica gel column chromatography (eluent: $CHCl_3$/*n*-hexane = 60:40), followed by HPLC. After vacuum drying at 60 °C for 2 h, ***(R)*-TPD** was obtained as a white solid (181.9 mg, 69% yield).

^{1}H NMR (600 MHz, $CDCl_3$): δ = 7.78 (s, 2H), 3.93 (dd, *J* = 10.2, 7.2 Hz, 1H), 2.02 (q, *J* = 11.4 Hz, 1H), 1.90 (d, *J* = 13.2 Hz, 1H), 1.76 (d, *J* = 13.8 Hz, 1H), 1.64 (t, *J* = 10.8 Hz, 2H), 1.56 (d, *J* = 13.8 Hz, 1H), 1.44 (d, *J* = 6.0 Hz, 3H), 1.27 (dd, *J* = 14.4, 12.0 Hz, 1H), 1.21-1.09 (m, 2H), 0.98-0.86 (m, 2H). ^{13}C{^{1}H} NMR (600 MHz, $CDCl_3$): δ = 162.88, 136.68, 125.22, 52.92, 39.82, 30.59, 30.19, 26.20, 25.87, 25.77, 16.24. EA: Found. C 63.68%, H 6.53%, N 5.25%, S 12.29%; Calcd. for $C_{14}H_{17}NO_2S$: C 63.85%, H 6.51%, N 5.32%, S 12.17%. APCI-TOF-MS: *m/z* Calcd. For $C_{14}H_{18}NO_2S$ ([M+H]) 264.1053, Found 264.1054 (Positive ion mode).

***(S)*-TPD** was synthesized in an analogous manner, affording the desired product as a white solid (160.1 mg, 61% yield). EA: Found. C 63.58%, H 6.51%, N 5.24%, S 12.24%;

Calcd. for $C_{14}H_{17}NO_2S$: C 63.85%, H 6.51%, N 5.32%, S12.17%. APCI-TOF-MS: *m/z* Calcd. For $C_{14}H_{18}NO_2S$ ([M+H]) 264.1053, Found 264.1027 (Positive ion mode).

Synthesis of **(*R*)-PFTPD**.

A 25 mL Schlenk tube equipped with a magnetic stir bar was charged with **(*R*)-TPD** (52.67 mg, 0.20 mmol), 2,7-dibromo-9,9-di-*n*-octylfluorene (109.70 mg, 0.20 mmol), and Cs_2CO_3 (165.33 mg, 0.51 mmol). Under a nitrogen atmosphere, a toluene solution of $Pd(PCy_3)_2$ (2.67 mg/mL) was added (1 mL, 4.0 μmol), followed by pivalic acid (6.9 μL, 0.060 mmol). The mixture was stirred at 100 °C for 24 h. After cooling to room temperature, the reaction mixture was dried under vacuum. The crude mixture was extracted with $CHCl_3$, and an aqueous solution of $NaS_2CN(C_2H_5)_2$ (1 mol%) was added (150 mL) and stirred overnight. The mixture was washed three times with distilled water and once with saturated brine. The organic layer was dried over Na_2SO_4 and concentrated under reduced pressure. The residue was subjected to reprecipitation from methanol and stirred overnight. The resulting solid was collected, washed with *n*-hexane, and dried under vacuum at 60 °C for 2 h to afford **(*R*)-PFTPD** as a yellow solid (122.6 mg, 94% yield).

^{1}H NMR (600 MHz, $CDCl_3$): δ = 8.29-8.18 (m, 4H), 7.86 (d, *J* = 8.4 Hz, 2H), 4.10 (br,

1H), 2.17 (br, 4H), 1.98 (br, 1H), 1.80 (br, 1H), 1.69 (br, 3H), 1.37-0.73 (br, 39H). $^{13}C\{^{1}H\}$ NMR (600 MHz, $CDCl_3$): δ = 163.22, 152.40, 145.13, 142.20, 130.55, 130.21, 127.62, 122.94, 120.62, 55.89, 53.01, 40.11, 39.85, 31.84, 30.76, 30.37, 30.04, 29.25, 29.21, 26.29, 25.98, 25.84, 24.00, 22.63, 16.38, 14.05. M_n = 45000, M_w/M_n = 2.1.

(*S*)-PFTPD was synthesized in an analogous manner, affording the desired product as a yellow solid (119.1 mg, 92% yield). M_n = 56000, M_w/M_n = 2.2.

ASSOCIATED CONTENT

Supporting Information.

The Supporting Information is available free of charge on the website.

Additional spectra (PDF), cif file.

Data availability statement.

The authors confirm that the data supporting the findings of this study are available within the article and its supplementary materials.

Notes

The authors report there are no competing interests to declare.

ACKNOWLEDGMENT

The authors thank the Chemical Analysis Center at the University of Tsukuba for NMR, the single-crystal X-ray diffraction, and mass spectrometry measurements. This work was partially supported by the Joint Usage/Research Project for Catalysis (No. 25DS0873 and 26DS0930). ZH acknowledges JST SPRING, Grant Number JPMJSP2124. WY acknowledges the Hirose and Kobayashi Foundation. RO acknowledges International Research Project on Chiral Field–Matter Interaction (IRP-ChiFiMI), the French National Research Agency under the France 2030 program (ANR-23-EXLU-0004, PEPR LUMA TORNADO), Core-to-Core program (JPJSCCA20250005), Grant-in-Aid for Scientific Research (B) (JP23H01782) from Japan Society for the Promotion of Science (JSPS) for

financial support. SK acknowledges Toyo Gousei foundation. YY acknowledges JST CREST (JPMJCR20T4) and KAKENHI (JP24H00470, JP24H01693) by JSPS.

References

[1] Watanabe K, Akagi K. Helically assembled π -conjugated polymers with circularly polarized luminescence. *Sci Technol Adv Mater*. 2014;15(4):044203 (1-21). doi:10.1088/1468-6996/15/4/044203

[2] Yamamoto Y, Yamagishi H, Huang JS, et al. Molecular and Supramolecular Designs of Organic/Polymeric Micro-photoemitters for Advanced Optical and Laser Applications. *Acc Chem Res*. 2023;56(12):1469-1481. doi:10.1021/acs.accounts.3c00084

[3] Albano G, Pescitelli G, Di Bari L. Chiroptical Properties in Thin Films of π-Conjugated Systems. *Chem Rev*. 2020;120(18):10145-10243. doi:10.1021/acs.chemrev.0c00195

[4] Wang N, Yu H, Zhong H, et al. Circularly polarized polymeric light-emitting diodes: preparation and properties. *Polym Chem*. 2025;16(4):396-408. doi:10.1039/D4PY00939H

[5] Ji MJ, Li M, Chen CF. Circularly polarized luminescence of macromolecular co-assembly systems. *Chem Sci*. 2025;16(27):12277-12292. doi:10.1039/d5sc02409a

[6] Fiesel R, Scherf U. Aggregation-induced CD effects in chiral poly(2,5-dialkoxy-1,4-phenylene)s. *Acta Polym*. 1998;49(8):445-449. doi:10.1002/(SICI)1521-4044(199808)49:8<445::AID-APOL445>3.0.CO;2-M

[7] Watanabe K, Sun Z, Akagi K. Interchain Helically π-Stacked Assembly of Cationic Chiral Poly(para-phenylene) Derivatives Enforced by Anionic π-Conjugated Molecules through Both Electrostatic and π–π Interactions. *Chem Mater*. 2015;27(8):2895-2902. doi:10.1021/acs.chemmater.5b00121

[8] Tanaka R, Yamaoka S, Ikeda S, et al. High-Intensity Circular Dichroism of Head-To-Tail Regioregular Poly(1,4-Phenylene)s in the Aggregated State. *Chem – A Eur J*. 2024;30(35):e202400706 (1-7). doi:10.1002/chem.202400706

[9] Peeters E, Delmotte A, Janssen RAJ, et al. Chiroptical properties of poly{2, 5-bis[(S)-2-methylbutoxy]-1, 4-phenylene vinylene}. *Adv Mater*. 1997;9(6):493-496. doi:10.1002/adma.19970090609

[10] Bouman MM, Meijer EW. Stereomutation in optically active regioregular polythiophenes. *Adv Mater*. 1995;7(4):385-387. doi:10.1002/adma.19950070408

[11] Otaki M, Komaba K, Goto H. Synthesis of Polythiophene-Based Chiral Magnetic Block Copolymers with High Stereoregularity. *ACS Appl Polym Mater*. 2023;5(1):311-319. doi:10.1021/acsapm.2c01524

[12] Oda M, Nothofer HG, Lieser G, et al. Circularly Polarized Electroluminescence from Liquid-Crystalline Chiral Polyfluorenes. *Adv Mater*. 2000;12(5):362-365. doi:10.1002/(SICI)1521-4095(200003)12:5<362::AID-ADMA362>3.0.CO;2-P

[13] Abbel R, Schenning APHJ, Meijer EW. Molecular weight optimum in the mesoscopic order of chiral fluorene (Co)polymer films. *Macromolecules*. 2008;41(20):7497-7504. doi:10.1021/ma8014855

[14] Lakhwani G, Gielen J, Kemerink M, et al. Intensive Chiroptical Properties of Chiral Polyfluorenes Associated with Fibril Formation. *J Phys Chem B*. 2009;113(43):14047-14051. doi:10.1021/jp903083x

[15] Watanabe K, Koyama Y, Suzuki N, et al. Gigantic chiroptical enhancements in polyfluorene copolymers bearing bulky neomenthyl groups: importance of alternating sequences of chiral and achiral fluorene units. *Polym Chem*. 2014;5(3):712-717. doi:10.1039/C3PY01442H

[16] Di Nuzzo D, Kulkarni C, Zhao B, et al. High Circular Polarization of Electroluminescence Achieved via Self-Assembly of a Light-Emitting Chiral Conjugated Polymer into Multidomain Cholesteric Films. *ACS Nano*. 2017;11(12):12713-12722. doi:10.1021/acsnano.7b07390

[17] Kulkarni C, Van Son MHC, Di Nuzzo D, et al. Molecular Design Principles for Achieving Strong Chiroptical Properties of Fluorene Copolymers in Thin Films. *Chem Mater*. 2019;31(17):6633-6641. doi:10.1021/acs.chemmater.9b00601

[18] Oki O, Kulkarni C, Yamagishi H, et al. Robust Angular Anisotropy of Circularly Polarized Luminescence from a Single Twisted-Bipolar Polymeric Microsphere. *J Am Chem Soc*. 2021;143(23):8772-8779. doi:10.1021/jacs.1c03185

[19] Nakayama S, Yamagishi H, Oki O, et al. Near-unity angular anisotropy of circularly polarized luminescence from microspheres of monodispersed chiral conjugated polymers. *Chem Commun*. 2024;60(59):7634-7637. doi:10.1039/D4CC01428F

[20] Zhao C, Yang F, Xia D, et al. Thieno[3,4-c]pyrrole-4,6-dione-based conjugated polymers for organic solar cells. *Chem Commun*. 2020;56(72):10394-10408. doi:10.1039/d0cc04150e

[21] Kushida S, Oki O, Saito H, et al. From Linear to Foldamer and Assembly: Hierarchical Transformation of a Coplanar Conjugated Polymer into a Microsphere. *J Phys Chem Lett*. 2017;8(18):4580-4586. doi:10.1021/acs.jpclett.7b02102

[22] Wakioka M, Ozawa F. Highly Efficient Catalysts for Direct Arylation Polymerization (DArP). *Asian J Org Chem*. 2018;7(7):1206-1216. doi:10.1002/ajoc.201800227

[23] Kuwabara J, Kanbara T. Facile Synthesis of π-Conjugated Polymers via Direct Arylation Polycondensation. *Bull Chem Soc Jpn*. 2019;92(1):152-161. doi:10.1246/bcsj.20180249

[24] Berrouard P, Najari A, Pron A, et al. Synthesis of 5-alkyl[3,4-*c*]thienopyrrole-4,6-dione-based polymers by direct heteroarylation. *Angew Chem, Int Ed*. 2012;51(9):2068-2071. doi:10.1002/anie.201106411

[25] Kuwabara J, Yamazaki K, Yamagata T, et al. The effect of a solvent on direct arylation polycondensation of substituted thiophenes. *Polym Chem*. 2015;6(6):891-895. doi:10.1039/C4PY01387E

[26] Kuwabara J, Fujie Y, Maruyama K, et al. Suppression of Homocoupling Side Reactions in Direct Arylation Polycondensation for Producing High Performance OPV Materials. *Macromolecules*. 2016;49(24):9388-9395. doi:10.1021/acs.macromol.6b02380

[27] Hu Z, Yasuda T, Kanbara T, et al. Synthesis of Conjugated Polymers with Controlled Terminal Structures by Direct Arylation Polycondensation and Correlation Between Terminal Structures and Emission Properties. *Macromol Chem Phys*. 2025;2025:2400506 (1–8). doi:10.1002/macp.202400506

[28] Sasaki Y, Gautier J, Li M, et al. Enhanced Chiral Exciton Coupling in Neat Molecular Films. *J Phys Chem C*. 2023;127(37):18526-18532. doi:10.1021/acs.jpcc.3c04212

[29] Hattori S, Vandendriessche S, Koeckelberghs G, V et al. Evaporation rate-based selection of supramolecular chirality. *Chem Commun*. 2017;53(21):3066-3069. doi:10.1039/C6CC09842H

[30] van Oosten A, Aerts K, de Coene Y, et al. Linking the Chiral Expression of Conjugated Polymers to Their Aggregation Type. *Macromolecules*. 2025;58(3):1390-1400. doi:10.1021/acs.macromol.4c02444

[31] Nielsen CB, Bjørnholm T. New regiosymmetrical dioxopyrrolo- and dihydropyrrolo-functionalized polythiophenes. *Org Lett*. 2004;6(19):3381-3384. doi:10.1021/ol048659n

[32] Yang S, Zhang S, Hu F, et al. Circularly polarized luminescence polymers: From design to applications. *Coord Chem Rev*. 2023;485:215116 (1-26). doi:10.1016/j.ccr.2023.215116

[33] Yan H, He Y, Wang D, et al. Aggregation-induced emission polymer systems with circularly polarized luminescence. *Aggregate*. 2023;4(4):e331(1-20). doi:10.1002/agt2.331

[34] Langeveld-Voss BMW, Janssen RAJ, Christiaans MPT, et al. Circular Dichroism and Circular Polarization of Photoluminescence of Highly Ordered Poly{3,4-di[(S)-2-methylbutoxy]thiophene}. *J Am Chem Soc*. 1996;118(20):4908-4909. doi:10.1021/ja9600643

[35] Satrijo A, Meskers SCJ, Swager TM. Probing a Conjugated Polymer's Transfer of Organization-Dependent Properties from Solutions to Films. *J Am Chem Soc*. 2006;128(28):9030-9031. doi:10.1021/ja063027c

[36] Watanabe K, Osaka I, Yorozuya S, et al. Helically π-Stacked Thiophene-Based Copolymers with Circularly Polarized Fluorescence: High Dissymmetry Factors Enhanced by Self-Ordering in Chiral Nematic Liquid Crystal Phase. *Chem Mater*. 2012;24(6):1011-1024. doi:10.1021/cm2028788

[37] Ikai T, Shimizu S, Awata S, et al. Synthesis and chiroptical properties of a π-conjugated polymer containing glucose-linked biphenyl units in the main chain capable of folding into a helical conformation. *Polym Chem*. 2016;7(48):7522-7529. doi:10.1039/C6PY01759B

[38] Wang Z, Liu S, Wang Y, et al. Tunable AICPL of (S)-Binaphthyl-Based Three-Component Polymers via FRET Mechanism. *Macromol Rapid Commun*. 2017;38(14):1700150 (1-6). doi:10.1002/marc.201700150

[39] Ma J, Wang Y, Li X, et al. Aggregation-induced CPL response from chiral binaphthyl-based AIE-active polymers via supramolecular self-assembled helical nanowires. *Polymer*. 2018;143:184-189. doi:10.1016/j.polymer.2018.04.006

[40] Ikai T, Takayama K, Wada Y, et al. Synthesis of a one-handed helical polythiophene: A new approach using an axially chiral bithiophene with a fixed: Syn -conformation. *Chem Sci*. 2019;10(18):4890-4895. doi:10.1039/c9sc00342h

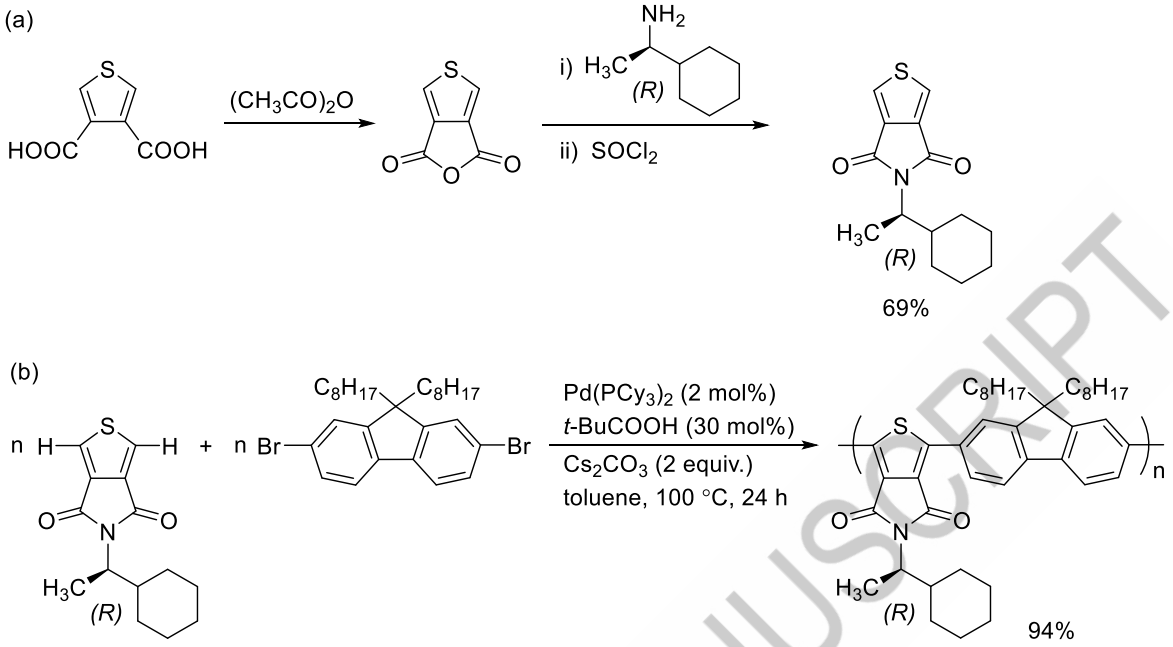

Scheme 1. (a) Synthesis of **(*R*)-TPD**; (b) synthesis of **(*R*)-PFTPD** *via* direct arylation polycondensation.

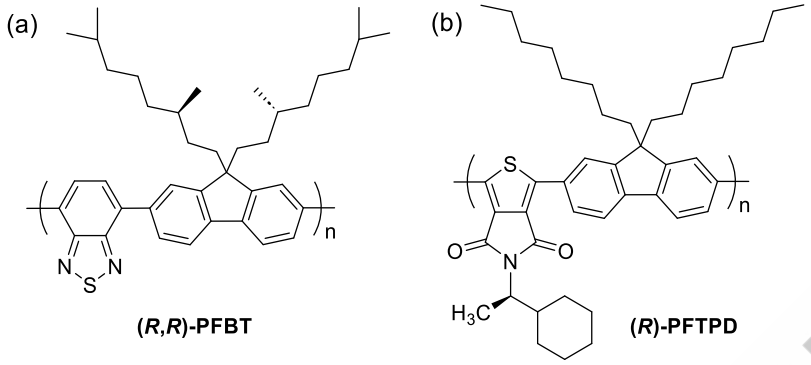

Figure 1. (a) Conventional fluorene-based chiral polymer **(*R*,*R*)-PFBT** and (b) the target polymer bearing a chiral TPD unit developed in this work **(*R*)-PFTPD**.

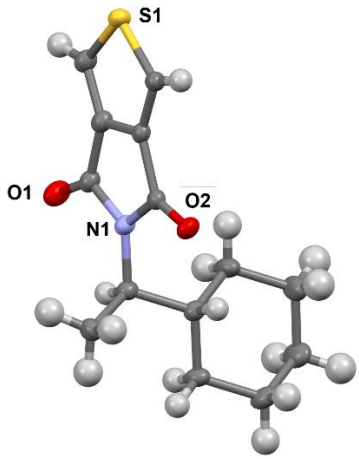

Figure 2. Crystal structure of **(*R*)-TPD** with thermal ellipsoids shown at the 50% probability level.

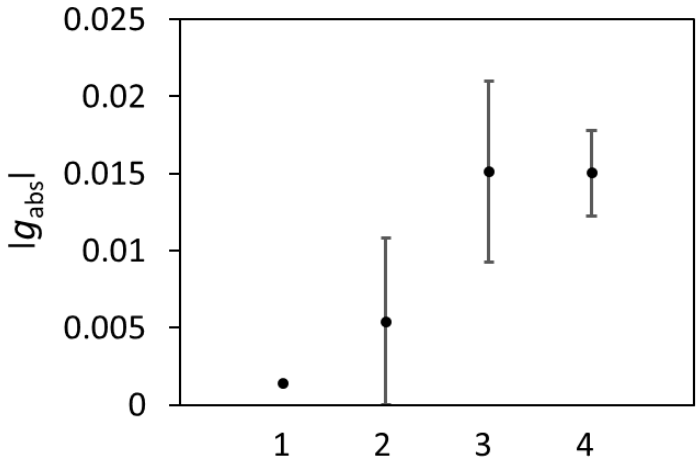

Figure 3. Dependence of the $|g_{abs}|$ values on the sample preparation conditions. Error bars represent the standard deviations obtained from repeated measurements. Details of conditions are shown in Table 2.

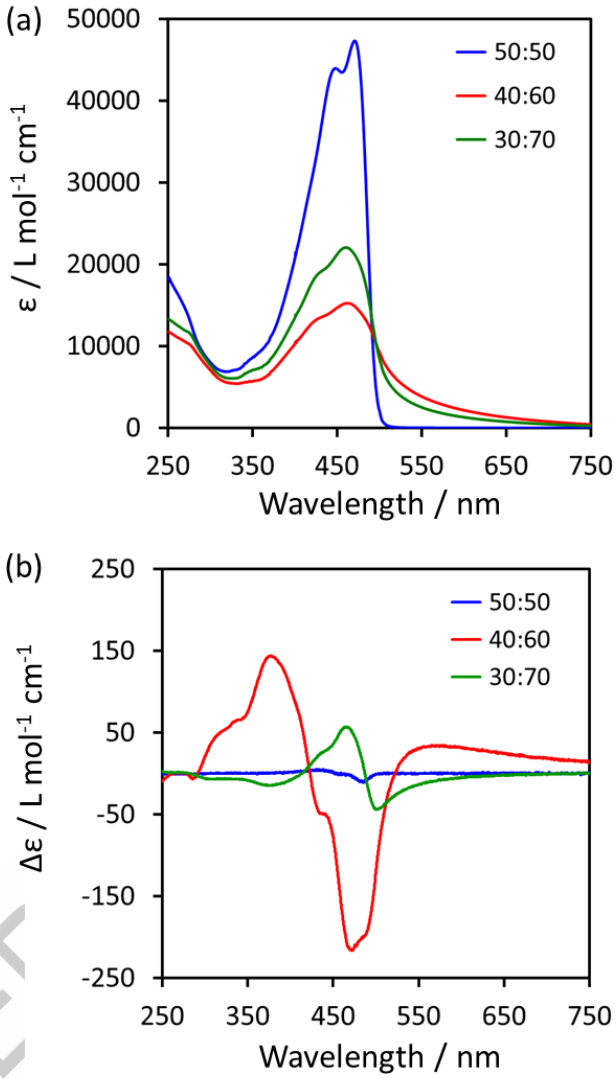

Figure 4. (a) UV–Vis absorption and (b) CD spectra of **(*R*)-PFTPD** recorded in $CHCl_3$/1-butanol mixtures with volume ratios of 50:50 (blue), 40:60 (red), and 30:70 (green) (3.0×10^{-5} M).

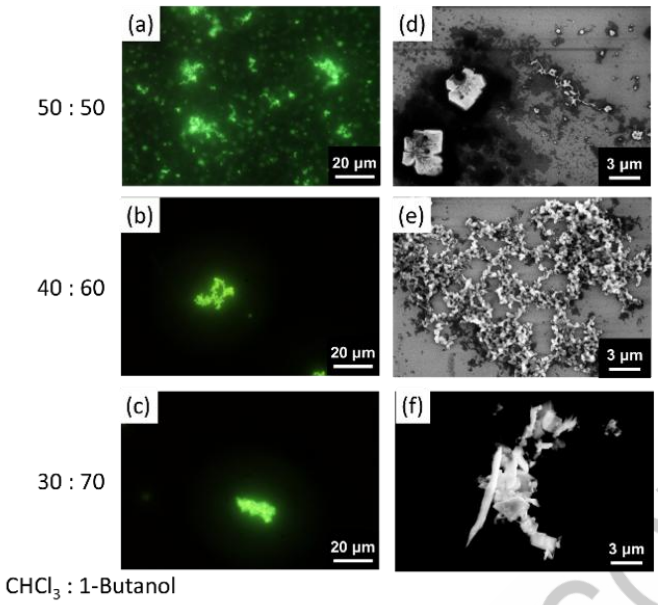

Figure 5. (a–c) Fluorescent microscopy images of the aggregates of **(*R*)-PFTPD** under blue–violet light irradiation in solvent mixtures of various ratios, and (d–f) SEM images of the samples prepared at each solvent ratio.

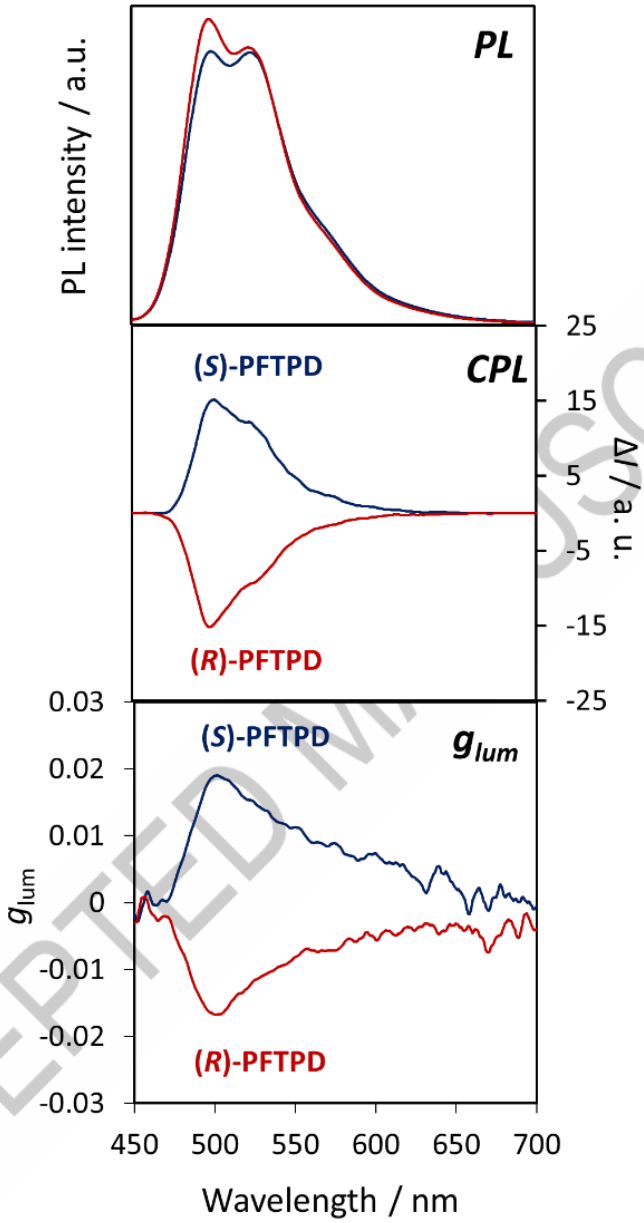

Figure 6. PL spectra, CPL spectra, and g_{lum} factors of **(*R*)-PFTPD** (red) and **(*S*)-PFTPD** (blue) recorded in $CHCl_3$/1-butanol mixtures with volume ratios of 40:60 (3.0×10^{-5} M, λ_{ex} = 400 nm).

Table 1. Results of polycondensation reactions and photophysical properties of the polymers in solution.

Polymer	Yield / %	M_n [a]	M_w/M_n [a]	λ_{abs} [b] / nm	λ_{em} [c] / nm	Φ [d] / %
***(R)*-PFTPD**	94	45,000	2.1	463	487	53
***(S)*-PFTPD**	92	56,000	2.2	463	487	53

[a] Estimated by GPC calibrated on polystyrene standards using $CHCl_3$ as an eluent at 40 °C. [b] Absorption maximum wavelength in $CHCl_3$ solution, [c] Emission maximum wavelength in $CHCl_3$ solution, [d] Photoluminescence quantum yield.

Table 2. Dependence of the $|g_{abs}|$ values on the sample preparation conditions [a]

Condition	Mixing method	Stirring speed	$\|g_{abs}\|$ [b]
1	Slow diffusion method [d]	Not applicable	0.0014 [c]
2	One-shot addition method [e]	Not applicable	0.0070 ± 0.0054
3	Stirring method [f]	Not specified	0.015 ± 0.0059
4	Stirring method [f]	450 rpm	0.015 ± 0.0028

[a] 1-BuOH (6 mL) was added to a 75 μM solution of **(*R*)-PFTPD** or **(*S*)-PFTPD** in $CHCl_3$ (4 mL).

[b] $|g_{abs}|$ values at the peak wavelengths around 480 nm (mean ± standard deviation)

[c] The standard deviation was not evaluated because the number of trials was insufficient.

[d] 1-Butanol was slowly poured into the polymer solution in $CHCl_3$, allowing the two solvents to diffuse gradually into each other.

[e] 1-Butanol was added all at once to the polymer solution in $CHCl_3$, followed by manual shaking to promote immediate mixing.

[f] 1-Butanol was added dropwise to the polymer solution in $CHCl_3$ under stirring.

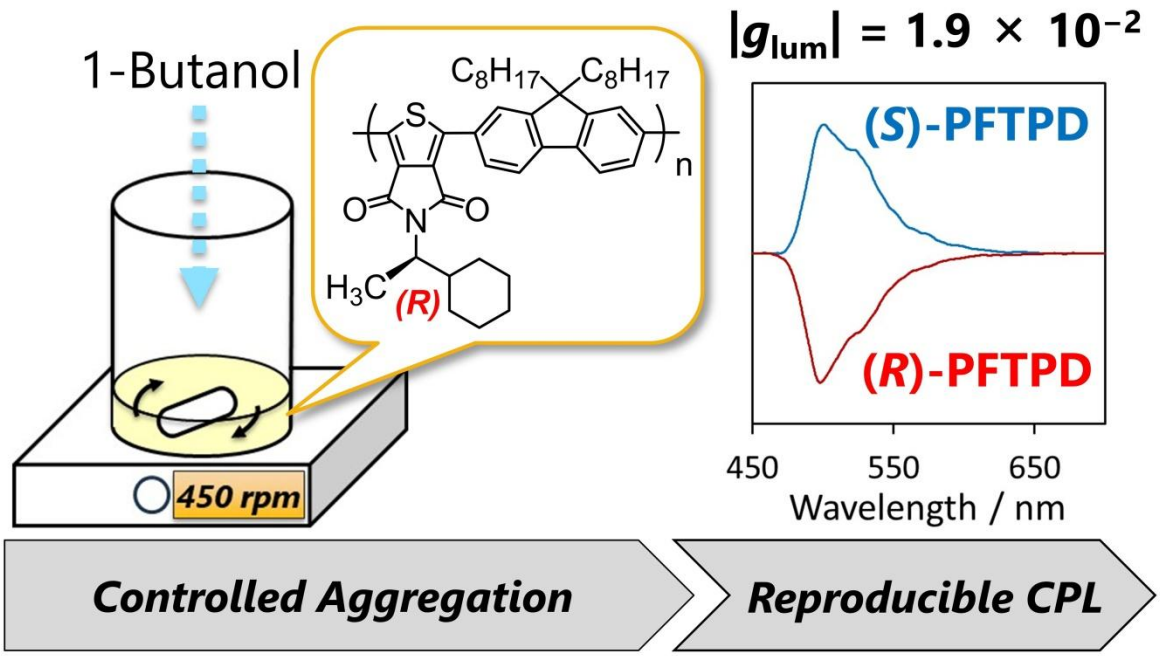

STAM_graphical_abstract_2

Impact Statement: This study demonstrates highly reproducible, strong CD and CPL from chiral π-conjugated polymers, enabled by a robust and standardized aggregate-formation protocol.

Impact Statement

Supporting information

Reproducible chiroptical activity from aggregated chiral thienopyrroledione–fluorene π-conjugated polymers.

Nao Suzuki,[a] Ziwei Hu,[a] Sota Nakayama,[a] Soh Kushida,[a] Yohei Yamamoto,[a,b] Wijak Yospanya,[c] Reiko Oda,[d,c] Takaki Kanbara,[a] Junpei Kuwabara[a,b] *

[a] *Institute of Pure and Applied Sciences, University of Tsukuba 1-1-1 Tennodai, Tsukuba, Ibaraki 305-8573, Japan.*

[b] *Tsukuba Research Center for Energy Materials Science (TREMS), Institute of Pure and Applied Sciences, University of Tsukuba, 1-1-1 Tennodai, Tsukuba, Ibaraki 305-8573, Japan.*

[c] *Advanced Institute for Materials Research (AIMR), Tohoku University, 2-1-1 Katahira, Aoba, Sendai, Miyagi, Japan*

[d] *University of Bordeaux, CNRS, Bordeaux INP, CBMN, UMR 5248, F-33600 Pessac, France*

E-mail: kuwabara@ims.tsukuba.ac.jp

(a)

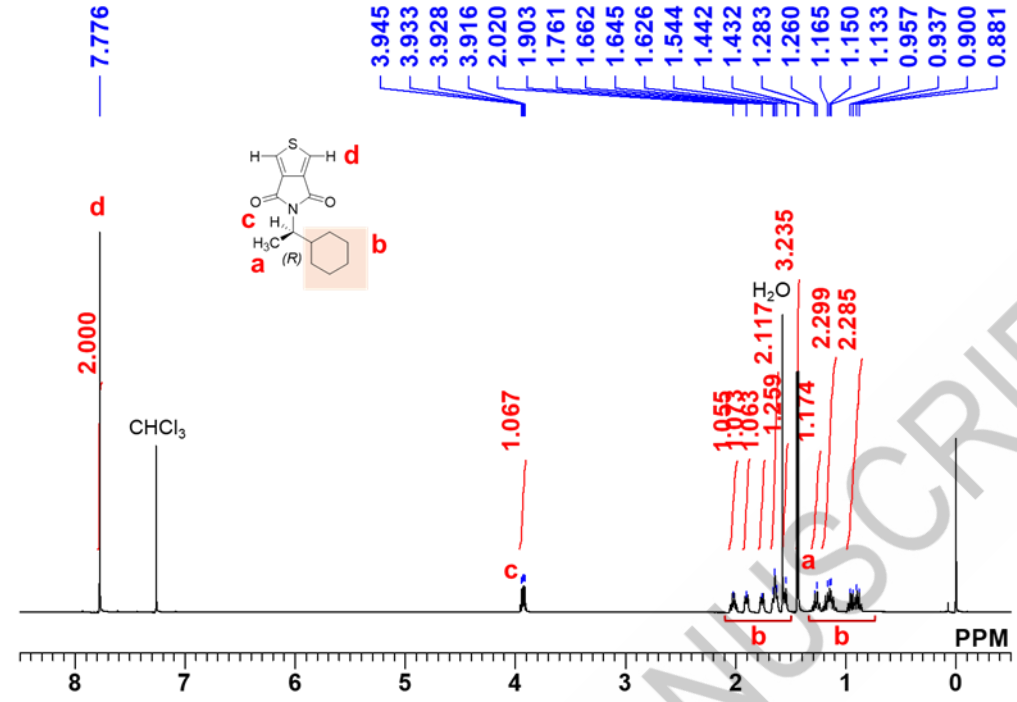

(b)

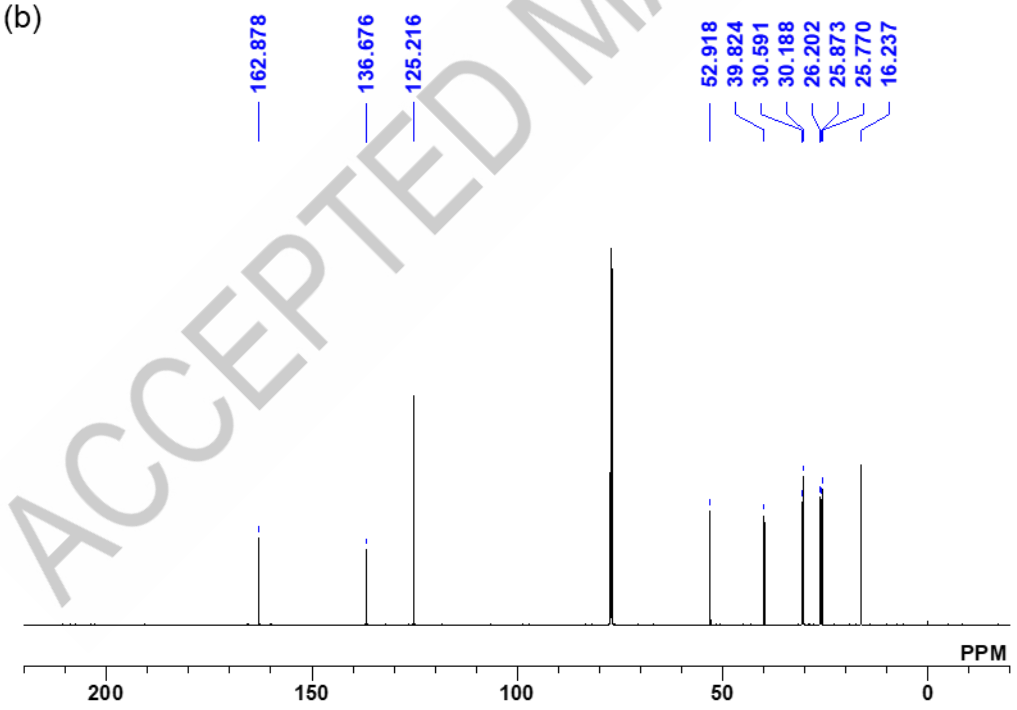

Figure S1. (a) ^{1}H NMR ($CDCl_3$, 600 MHz, r.t.) and (b) $^{13}C\{^{1}H\}$ NMR spectrum of ***(R)*-TPD** ($CDCl_3$, 150 MHz, r.t.).

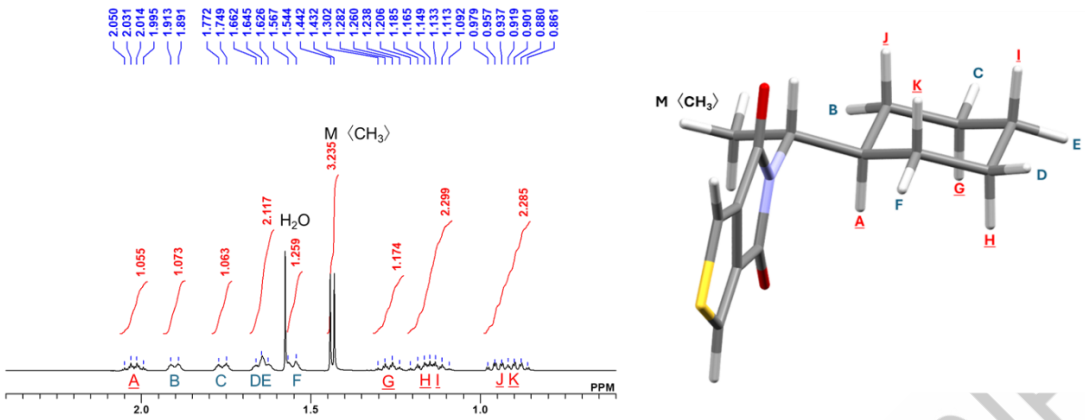

Figure S2. ^{1}H NMR spectrum of ***(R)*-TPD** ($CDCl_3$, 600 MHz, r.t., 0.6-2.4 ppm)

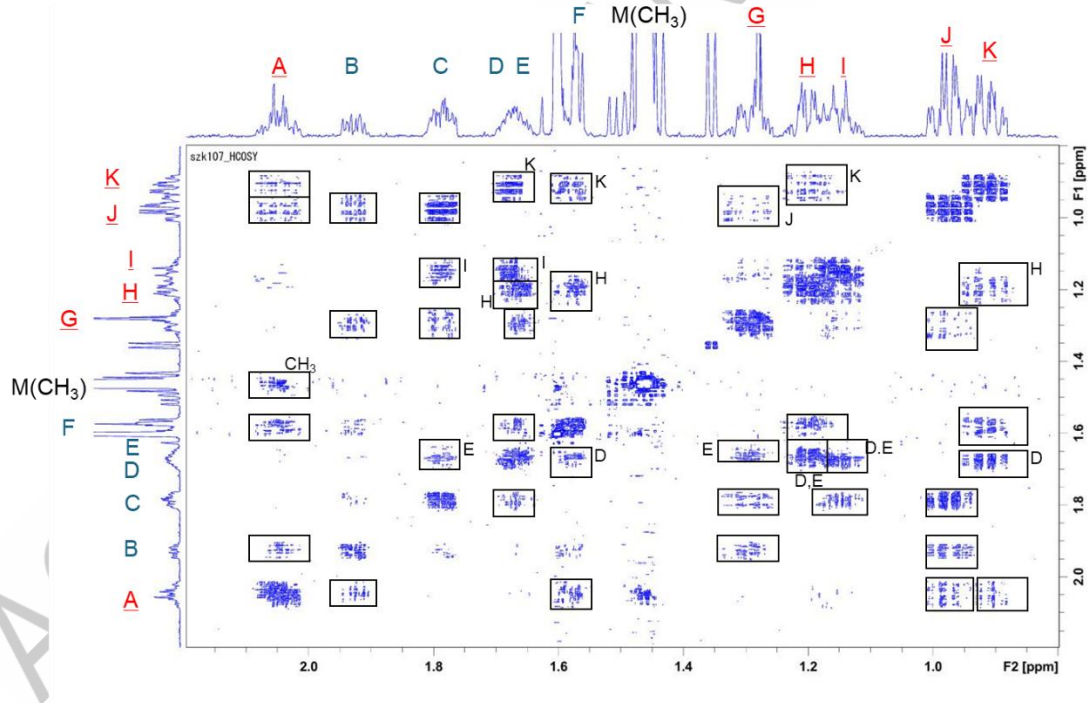

Figure S3. ^{1}H-^{1}H COSY spectrum of ***(R)*-TPD** ($CDCl_3$, 600 MHz, r.t., 0.6-2.4 ppm).

(a)

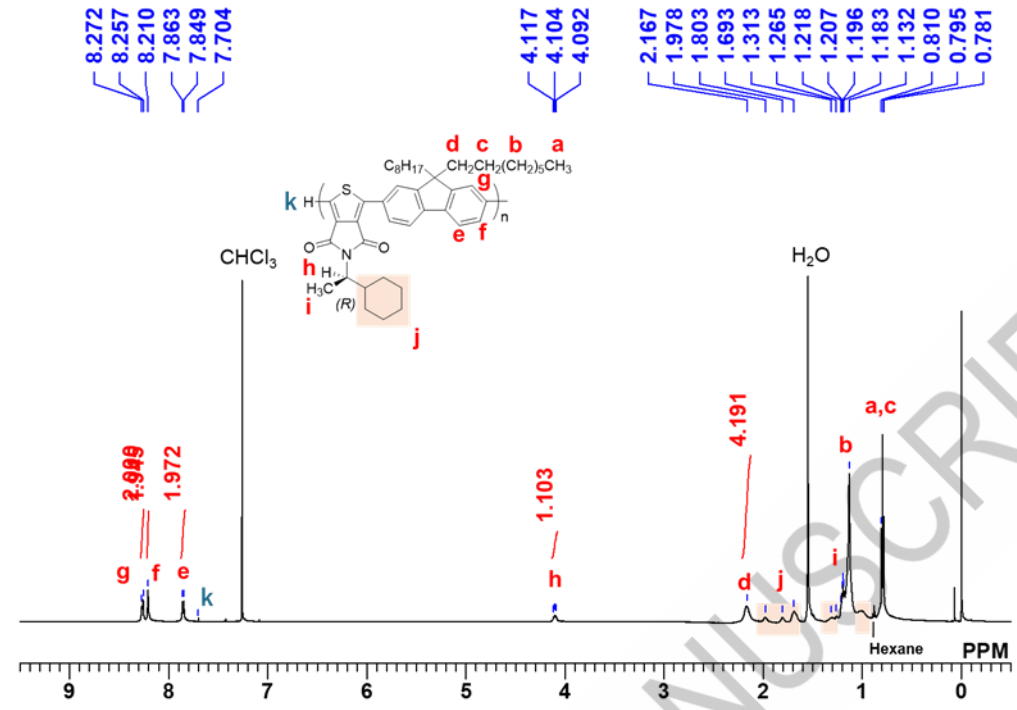

(b)

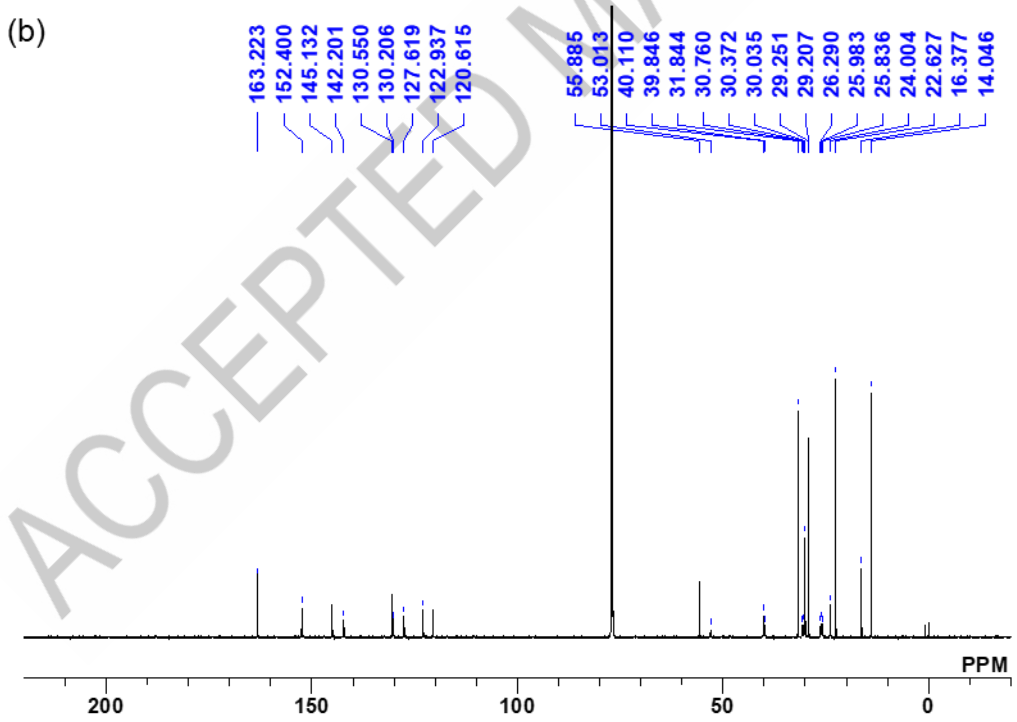

Figure S4. (a) ^{1}H NMR ($CDCl_3$, 600 MHz, r.t.) and (b) $^{13}C\{^{1}H\}$ NMR spectra of ***(R)*-PFTPD** ($CDCl_3$, 150 MHz, r.t.).

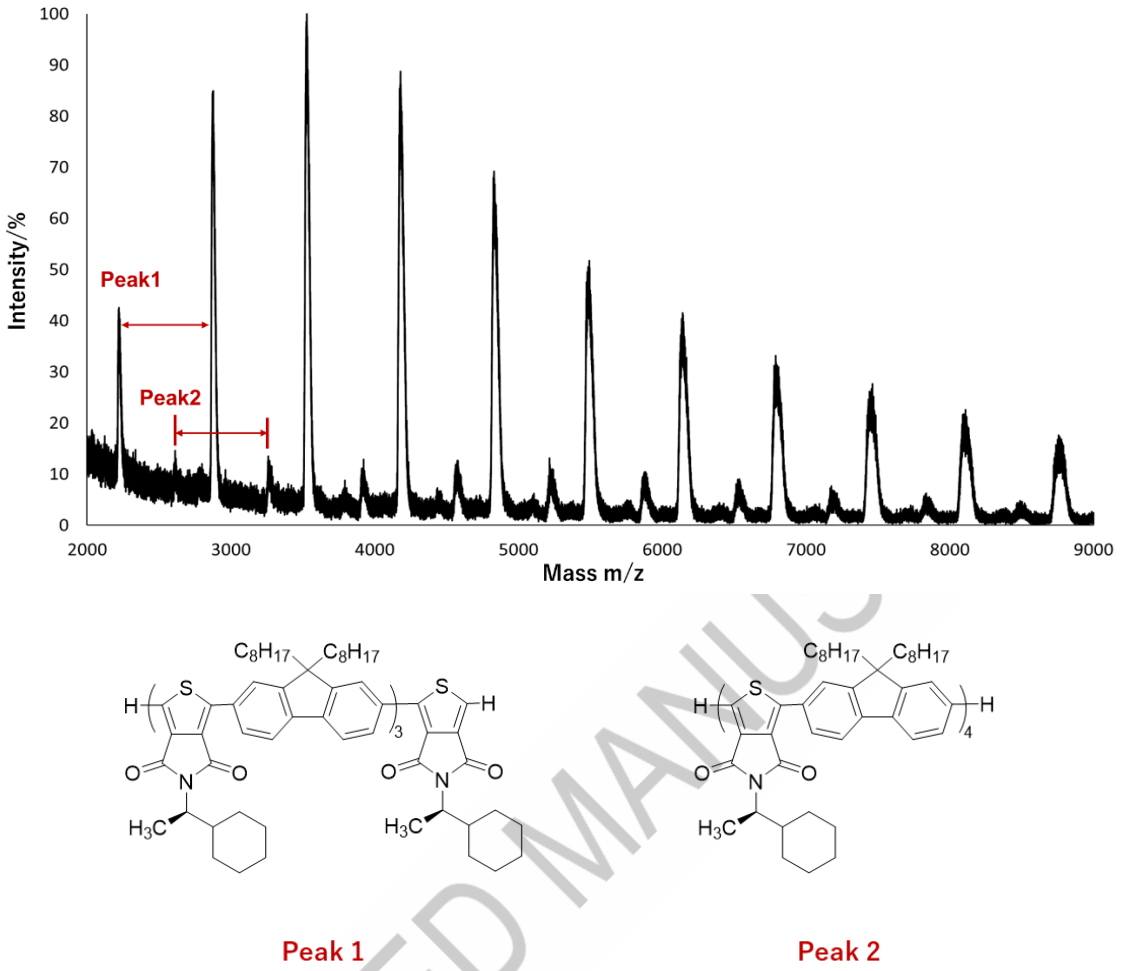

Figure S5. MALDI-TOF-MS spectrum of ***(R)*-PFTPD**.

(a)

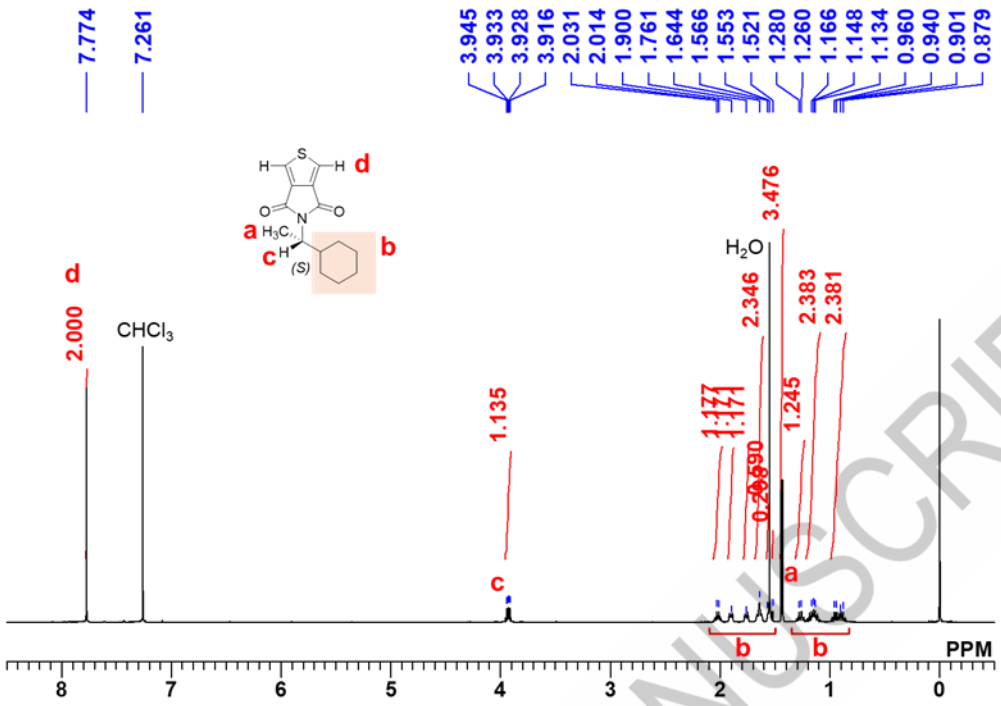

(b)

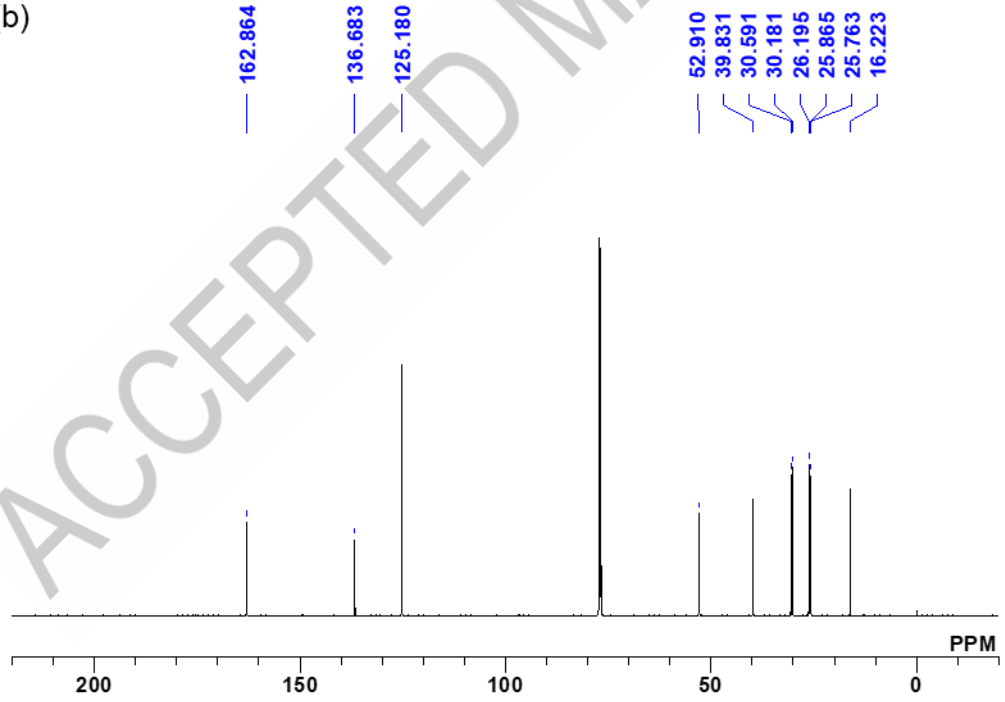

Figure S6. (a) ^{1}H NMR ($CDCl_3$, 600 MHz, r.t.) and (b) $^{13}C\{^{1}H\}$ NMR spectra of ***(S)*-TPD** ($CDCl_3$, 150 MHz, r.t.).

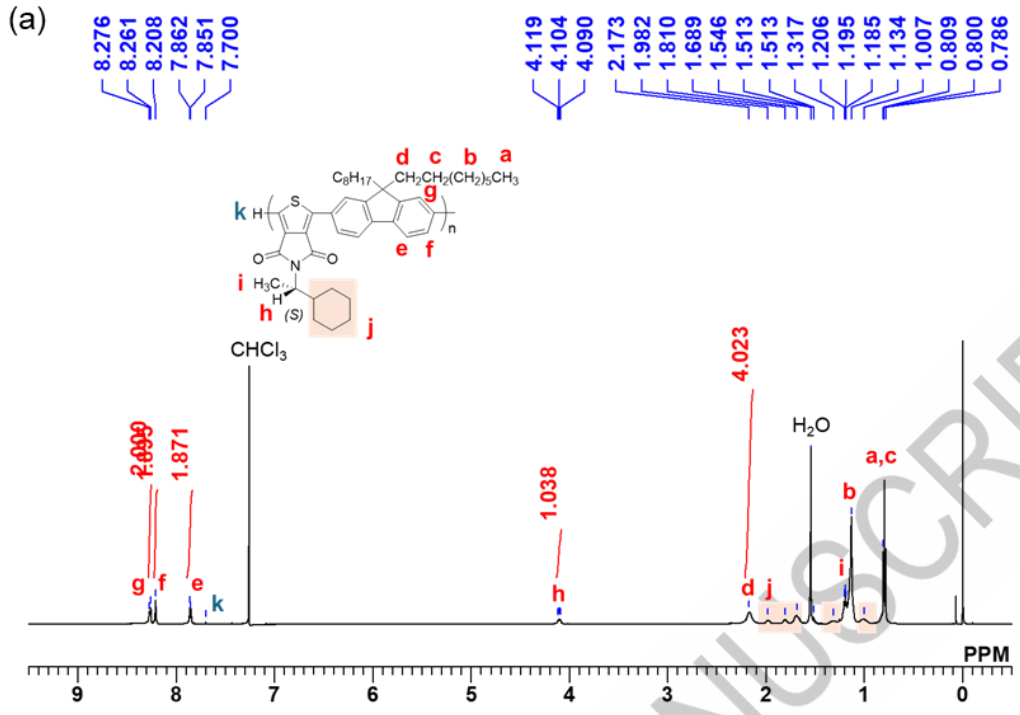

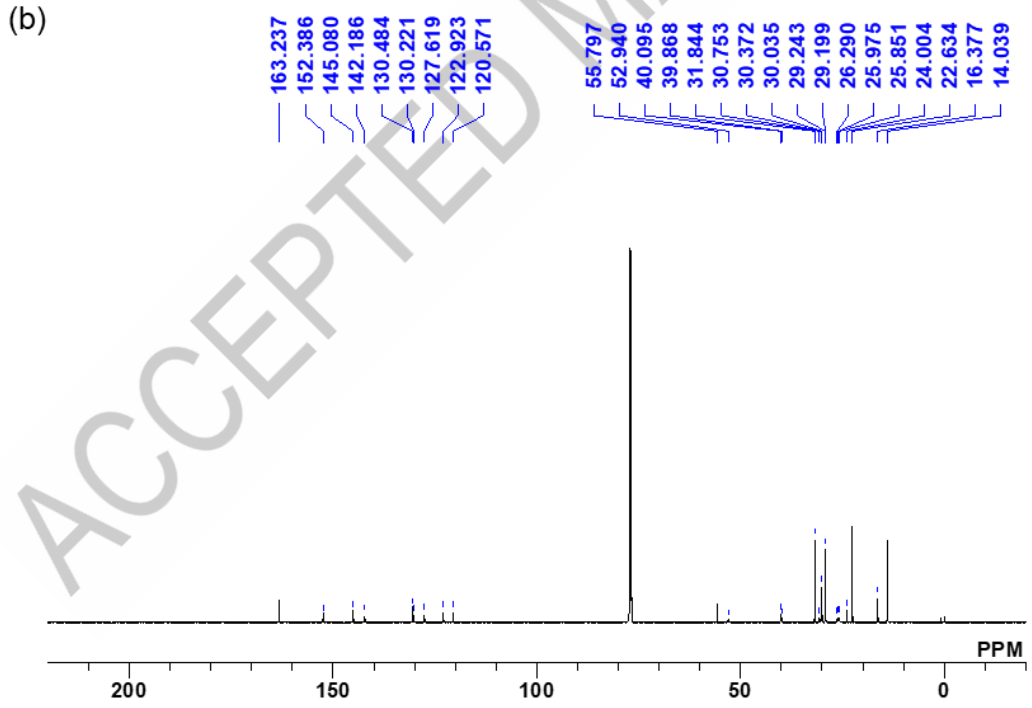

Figure S7. (a) ^{1}H NMR ($CDCl_3$, 600 MHz, r.t.) and (b) $^{13}C\{^{1}H\}$ NMR spectra of **(*S*)-PFTPD** ($CDCl_3$, 150 MHz, r.t.).

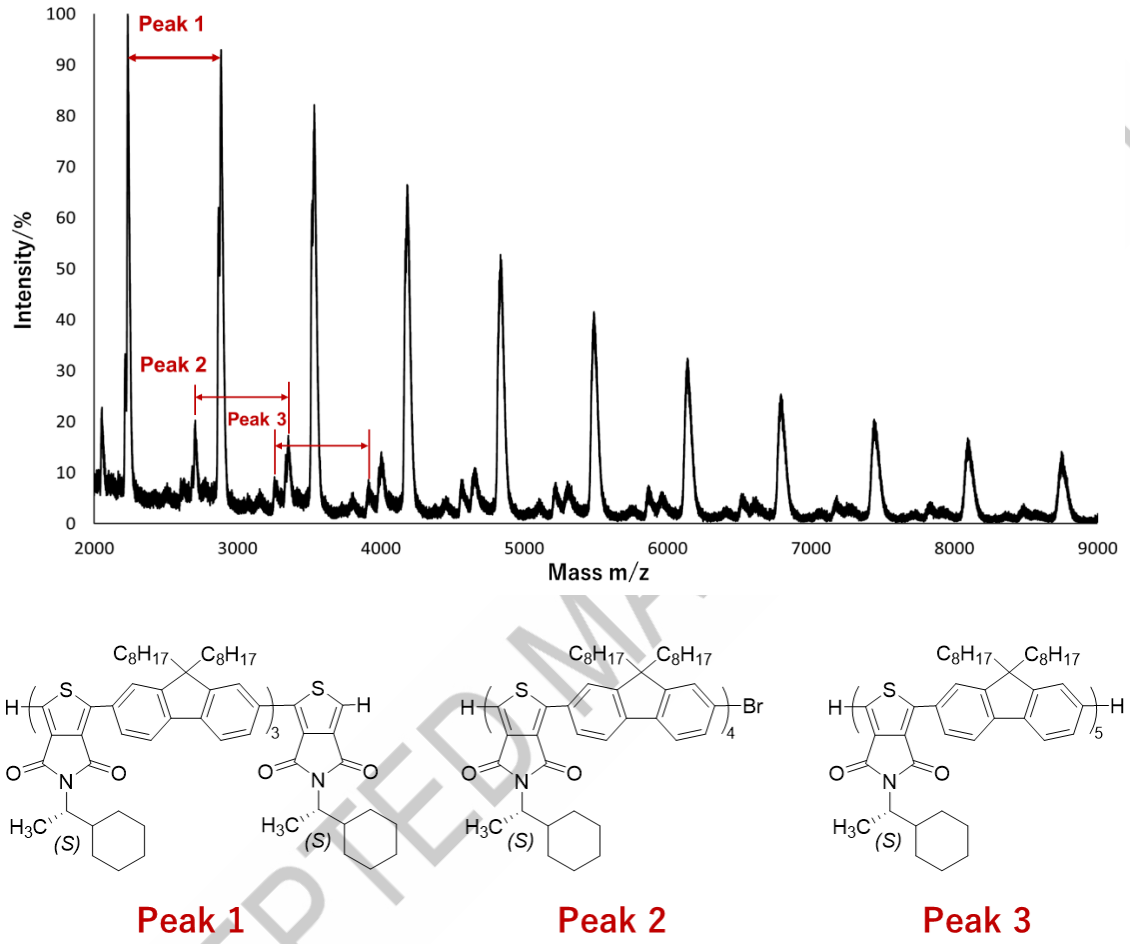

Figure S8. MALDI-TOF-MS spectrum of **(*S*)-PFTPD**.

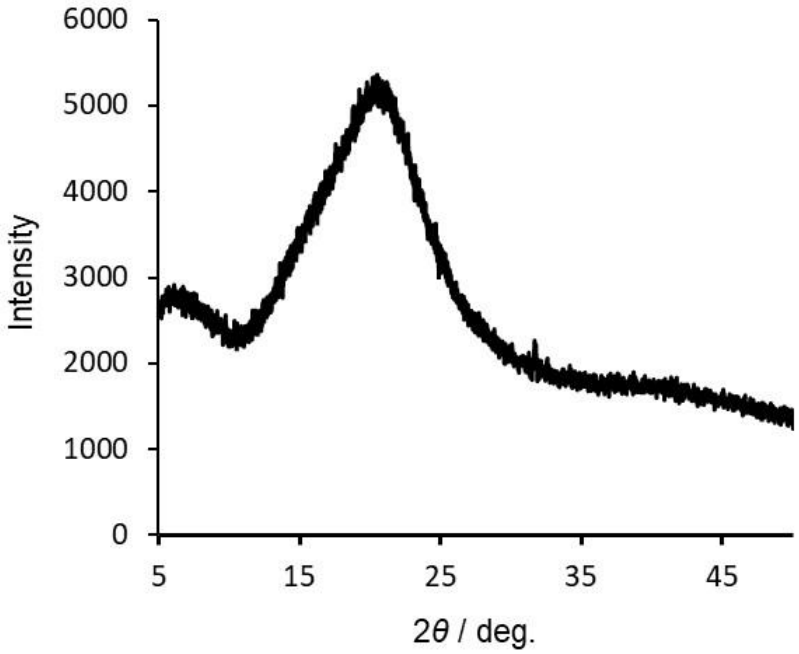

Figure S9. X-ray diffraction (XRD) patterns of a cast film of **(*R*)-PFTPD** measured using Cu*K*α radiation at room temperature.

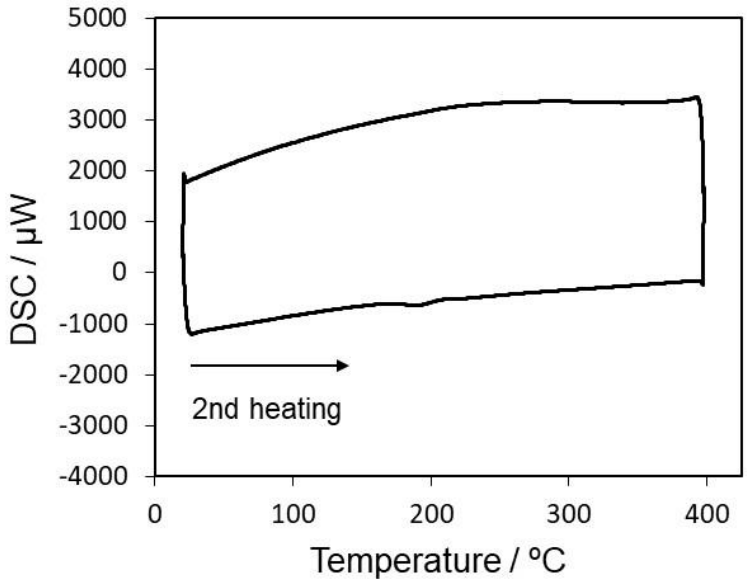

Figure S10. DSC thermograms of **(*R*)-PFTPD** measured under an Ar atmosphere at a heating rate of 10 K min^{-1} using a sample mass of 4.43 mg. The second heating scan after erasing the thermal history is shown.

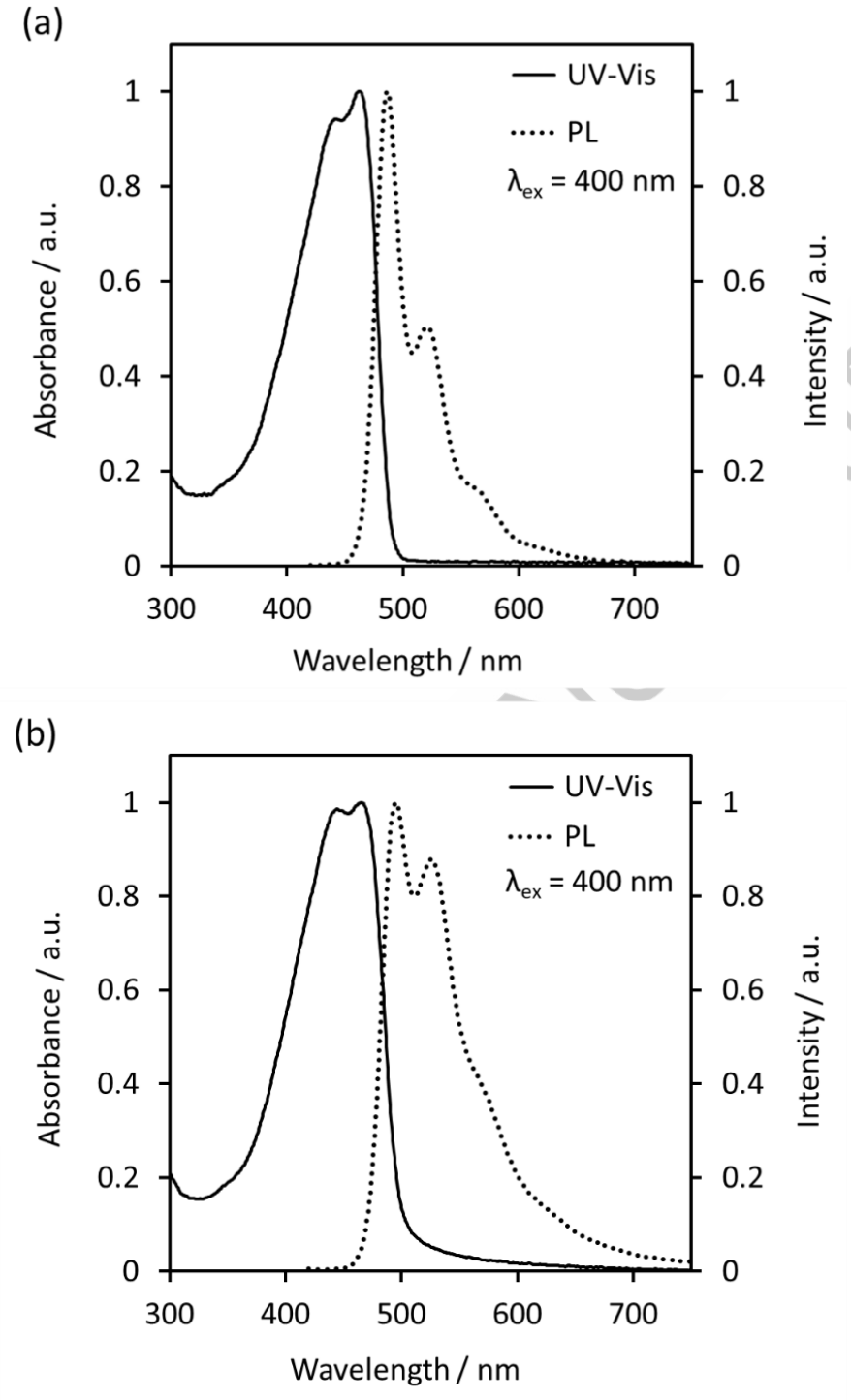

Figure S11. UV-Vis absorption and photoluminescence spectra of **(*R*)-PFTPD** (a) in solution state ($CHCl_3$, 5.0×10^{-6} M) and (b) in thin film state.

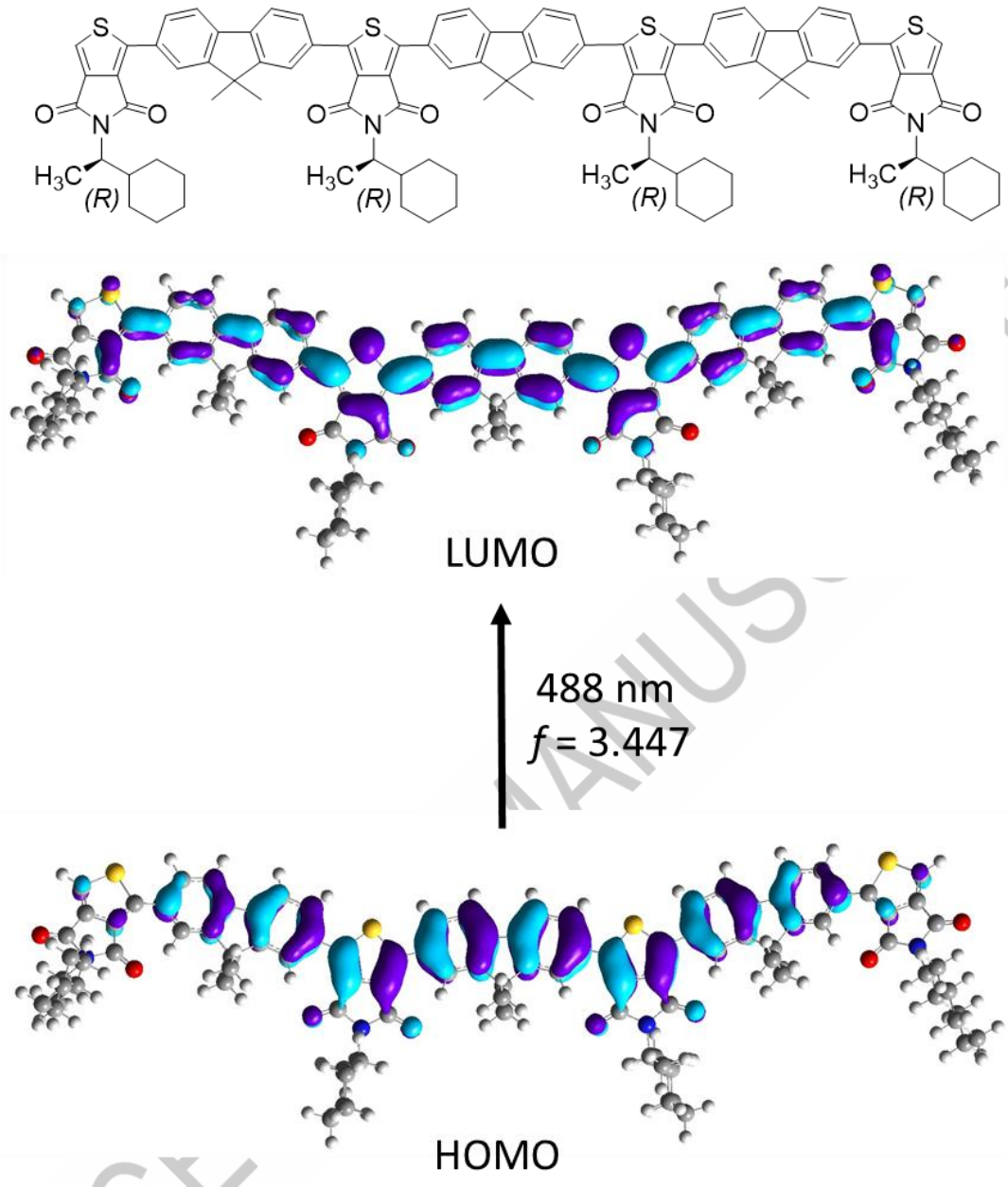

Figure S12. Frontier molecular orbitals (HOMO and LUMO), along with the predicted absorption wavelengths and corresponding oscillator strengths (*f*) obtained from a TD-DFT calculation.

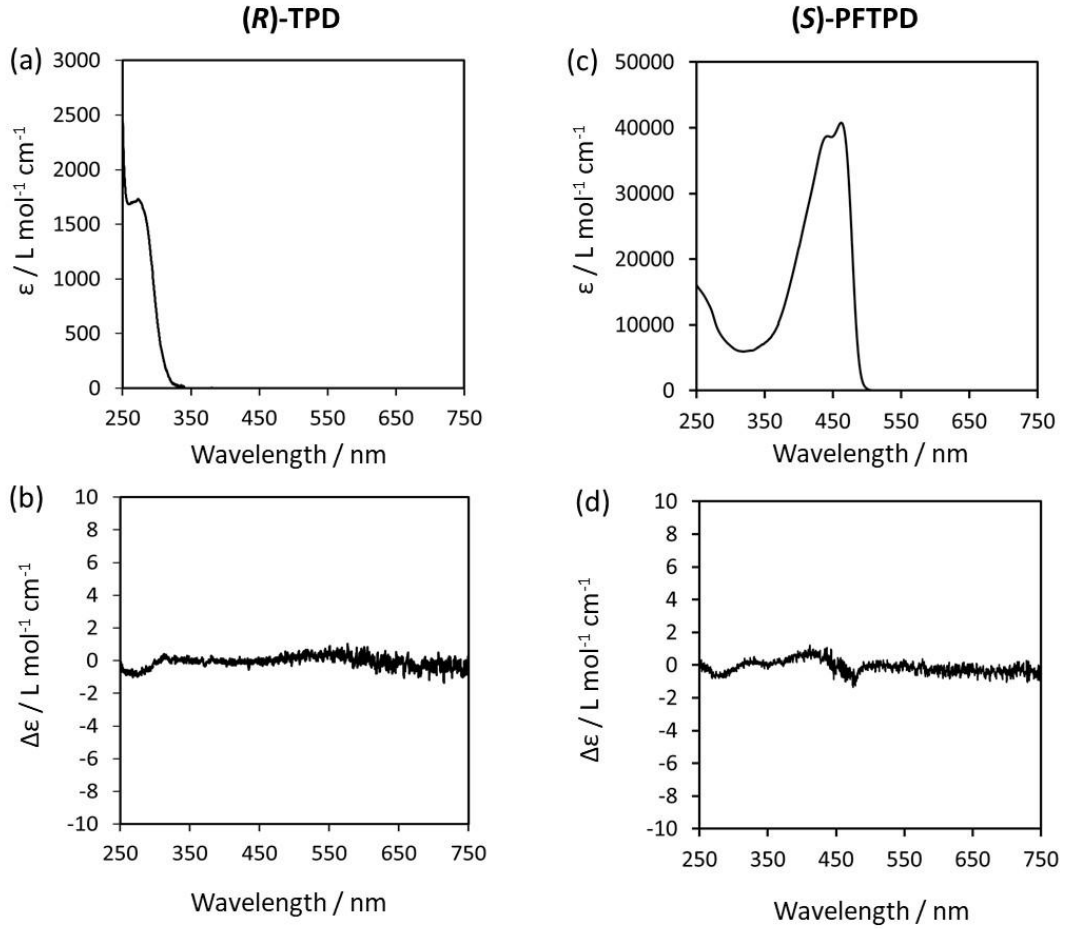

Figure S13. (a) UV–Vis absorption, (b) CD spectra of **(*R*)-TPD**, (c) UV–Vis absorption, and (d) CD spectra of **(*R*)-PFTPD** recorded in $CHCl_3$ (3.0×10^{-5} M).

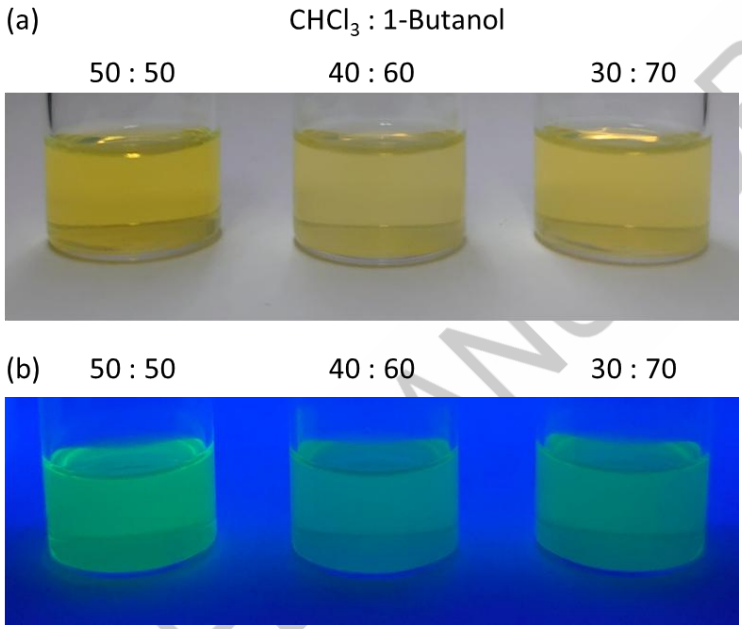

Figure S14. Photographs of **(*R*)-PFTPD** in the different solvent mixtures under natural light and under UV light (365 nm) illumination.

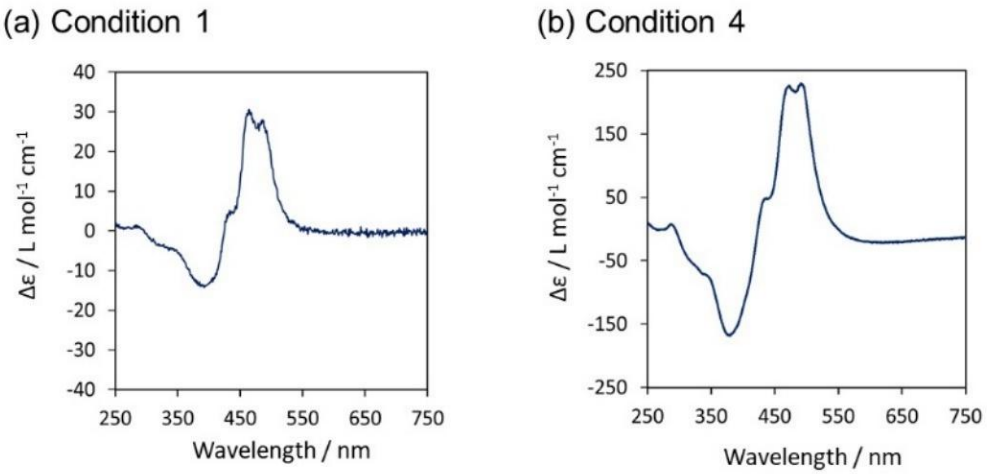

Figure S15. CD spectra of **(*S*)-PFTPD** aggregates prepared under different mixing conditions: (a) Condition 1 and (b) Condition 4. Figure (a) corresponds to the sample listed as Entry 2 in Table S1, while figure (b) corresponds to the sample listed as Entry 30 in Table S1. The spectra were recorded for samples of **(*S*)-PFTPD** in $CHCl_3$/1-butanol mixtures with a volume ratio of 40:60 (3.0×10^{-5} M).

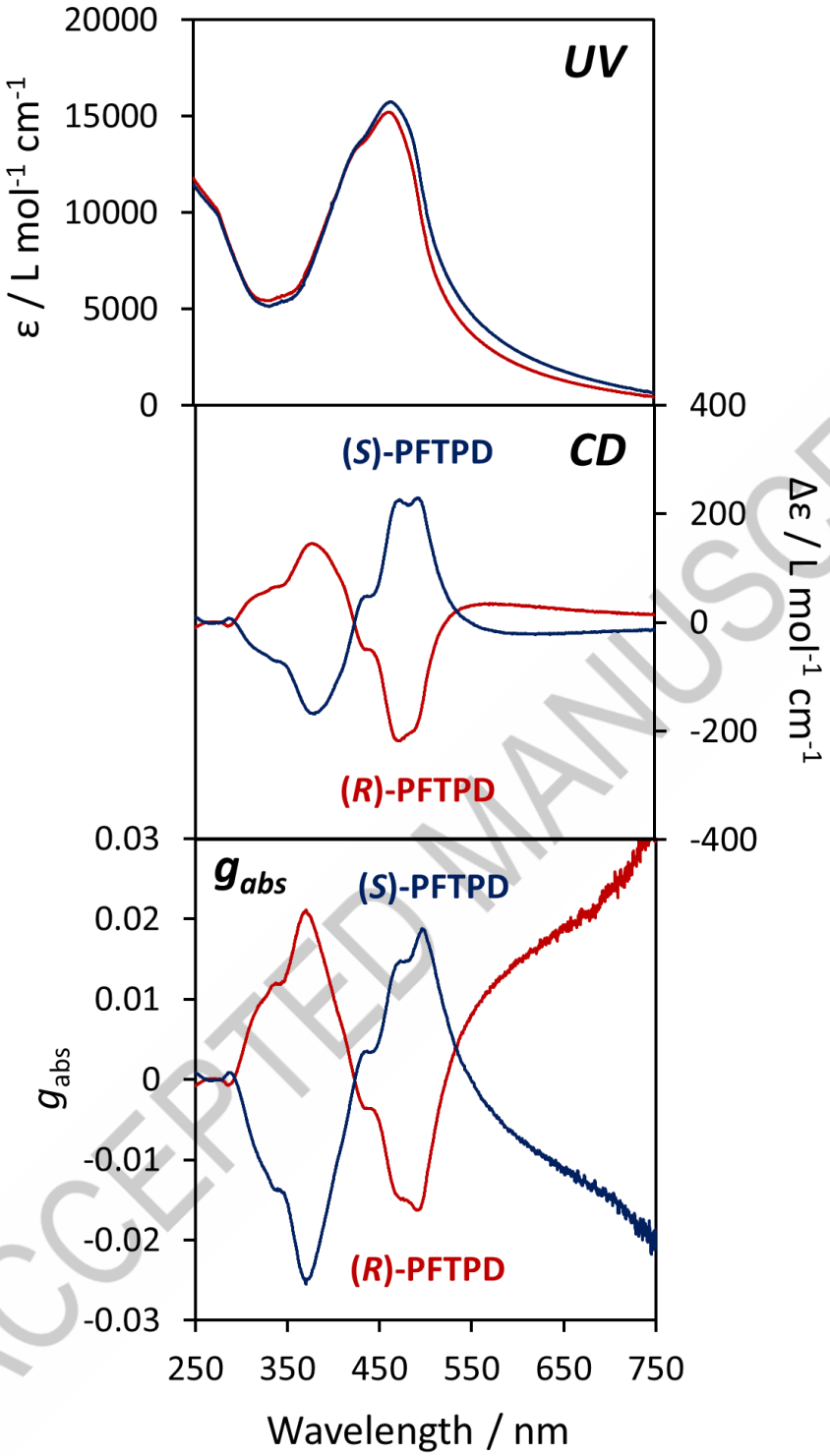

Figure S16. UV-Vis absorption spectra, CD spectra, and g_{abs} factors of **(*R*)-PFTPD** (red) and **(S)-PFTPD** (blue) recorded in $CHCl_3$/1-butanol mixtures with volume ratios of 40:60 (3.0×10^{-5} M).

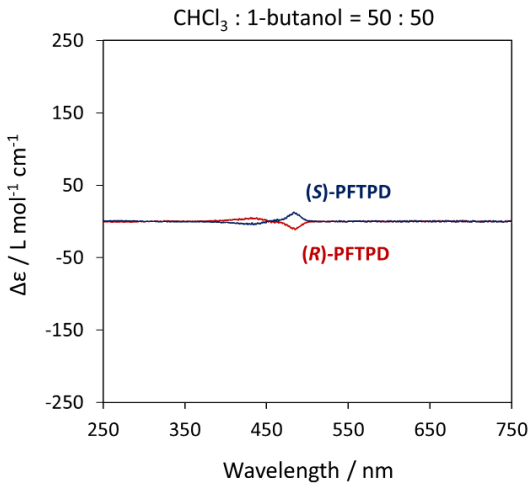

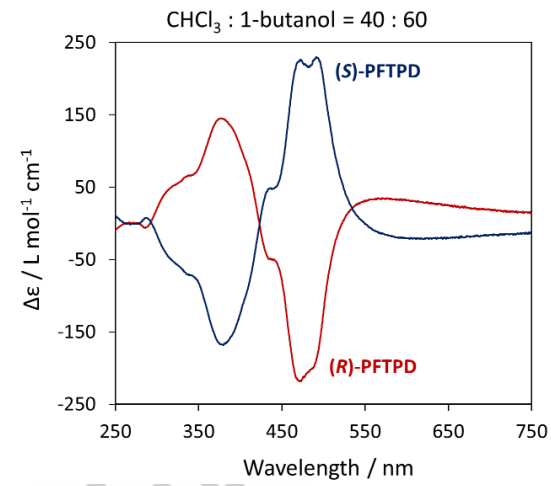

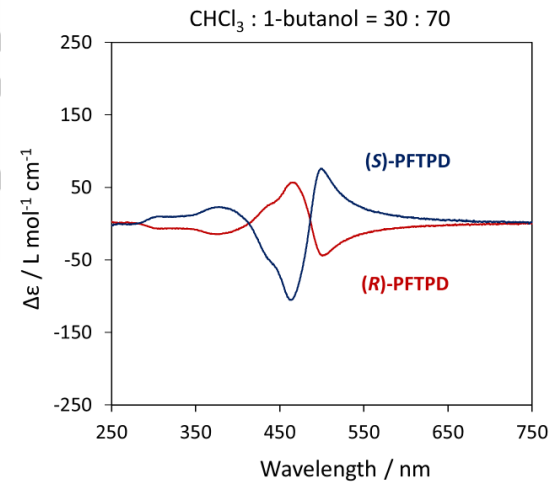

Figure S17. CD spectra of **(*R*)-PFTPD** (red) and **(*S*)-PFTPD** (blue) recorded in $CHCl_3$/1-butanol mixtures with volume ratios of 50:50, 40:60, and 30:70 (3.0×10^{-5} M).

Table S1. Original g_{abs} values corresponding to the preparation conditions. [a]

Entry	Condition	*R* or *S*	g_{abs} [f]
1	1 [b]	*S*	0.0000874
2		*S*	0.00266
3	2 [c]	*S*	0.00595
4		*S*	0.00231
5		*S*	0.0165
6		*S*	0.0128
7		*S*	0.00343
8		*R*	−0.00513
9		*R*	−0.00349
10	3 [d]	*S*	0.0186
11		*S*	0.0173
12		*S*	0.0127
13		*S*	0.0151
14		*S*	0.0277
15		*S*	0.0202
16		*S*	0.0234
17		*S*	0.0158
18		*S*	0.00935
19		*R*	−0.00540
20		*R*	−0.00770
21		*R*	−0.0188
22		*R*	−0.0152
23		*R*	−0.0127
24		*R*	−0.0100
25		*R*	−0.0118
26	4 [e]	*S*	0.0114
27		*S*	0.0116
28		*S*	0.0132
29		*S*	0.0142
30		*S*	0.0181

31	*R*	−0.0150
32	*R*	−0.0190
33	*R*	−0.0153
34	*R*	−0.0175

[a] 1-BuOH (6 mL) was added to a 75 μM solution of **(*R*)-PFTPD** or **(*S*)-PFTPD** in $CHCl_3$ (4 mL). The conditions are shown in Table 2.

[b] 1-Butanol was slowly poured into the polymer solution in $CHCl_3$, allowing the two solvents to diffuse gradually into each other.

[c] 1-Butanol was added all at once to the polymer solution in CHC_3, followed by manual shaking to promote immediate mixing.

[d] 1-Butanol was added dropwise to the polymer solution in $CHCl_3$ under stirring.

[e] 1-Butanol was added dropwise to the polymer solution in $CHCl_3$ under stirring (450 rpm).

[f] g_{abs} values at the peak wavelengths around 480 nm.

Table S2. Representative g_{abs} values of **(*R*)-PFTPD**. [a]

Solvent ratio $CHCl_3$: 1-butanol	g_{abs}	Wavelength
100 : 0	~ 0	-

50 : 50	-4.2×10^{-4}	485
40 : 60	-1.6×10^{-2}	491
30 : 70	-6.8×10^{-3}	513

[a] g_{abs} values calculated from the data shown in Figures 3 and S11.

Table S3. Original g_{lum} values. [a]

R or *S*	g_{lum}
S	0.0239
S	0.0190
S	0.0127
R	−0.0256
R	−0.0168
R	−0.0158

[a] g_{lum} values **(*R*)-PFTPD** and **(*S*)-PFTPD** recorded in $CHCl_3$/1-butanol mixtures with volume ratios of 40:60 (3×10^{-5} M, λ_{ex} = 400 nm).